WYOMING STATE GEOLOGICAL SURVEY
Thomas A. Drean, Director and State Geologist
Laramie, Wyoming

Interpreting the past, providing for the future

OPEN FILE REPORT 2017-5
Fort Steele 1:24,000-scale
Bedrock Geologic Map

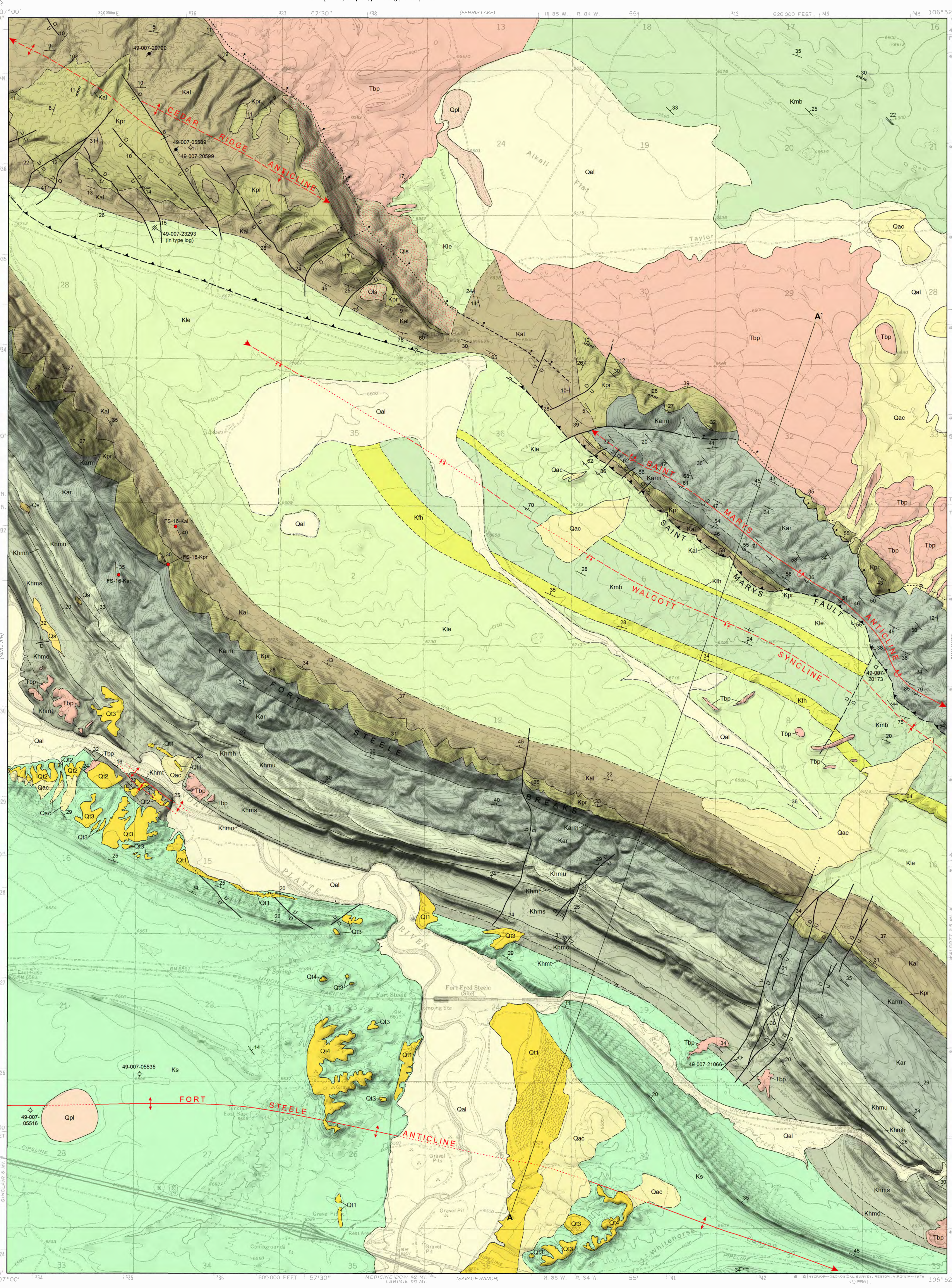

Base map from U.S. Geological Survey 1:24,000-scale topographic map of the Fort Steele, Wyoming Quadrangle, 1971

Base hillshade derived from USDA/NRCS–National Cartography & Geospatial Center 10-meter Digital Elevation Model (DEM), 2000; azimuth 315º, sun angle 45º, vertical exaggeration 3.0

Projection: Universal Transverse Mercator (UTM), zone 13
North American Datum of 1927 (NAD 27)
1,000-meter grid ticks: UTM, zone 13
10,000-foot grid ticks: Wyoming State Plane Coordinate System, east central zone

Wyoming State Geological Survey
P.O. Box 1347 - Laramie, WY 82073-1347
Phone: 307-766-2286 - Fax: 307-766-2605
Email: wsgs-info@wyo.gov

MN
GN
1°17'
9°27'
UTM GRID AND (2017) MAGNETIC NORTH DECLINATION AT CENTER OF SHEET

SCALE 1:24,000

1 0.5 0 1 Mile
1,000 0 1,000 2,000 3,000 4,000 5,000 6,000 7,000 Feet
1 0.5 0 1 Kilometer

CONTOUR INTERVAL 20 FEET
NATIONAL GEODETIC VERTICAL DATUM OF 1929

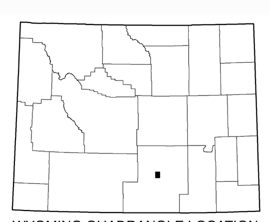

WYOMING QUADRANGLE LOCATION

Digital cartography by Jackie M. Wrage and Ranie M. Lynds

Map edited by Suzanne C. Luhr

Prepared in cooperation with and research supported by the U.S. Geological Survey, National Cooperative Geologic Mapping Program, under USGS award number G16AC00199. The views and conclusions contained in this document are those of the authors and should not be interpreted as necessarily representing the official policies, either expressed or implied, of the U.S. Government.

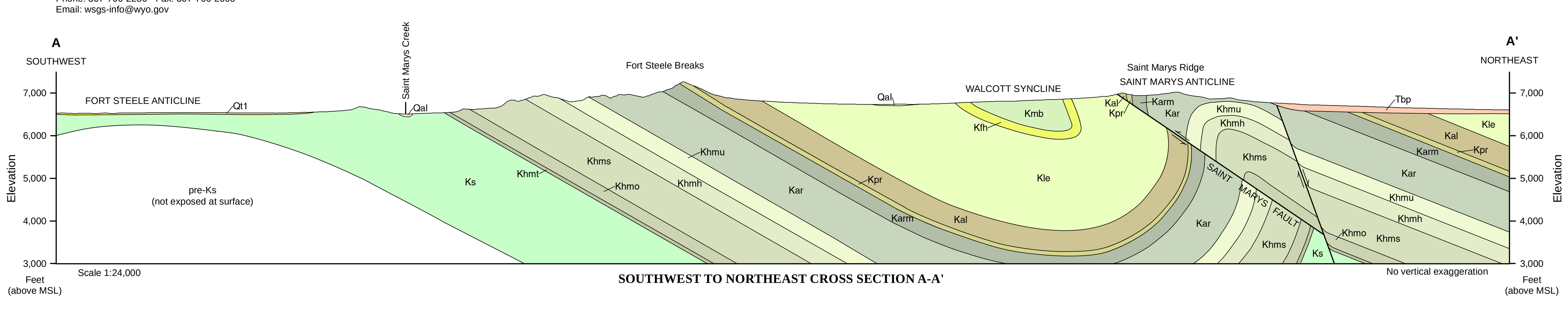

Scale 1:24,000
SOUTHWEST TO NORTHEAST CROSS SECTION A-A'
No vertical exaggeration

PRELIMINARY GEOLOGIC MAP OF THE FORT STEELE QUADRANGLE, CARBON COUNTY, WYOMING

by

Ranie M. Lynds and Jackie M. Wrage

2017

EXPLANATION

CORRELATION OF MAP UNITS

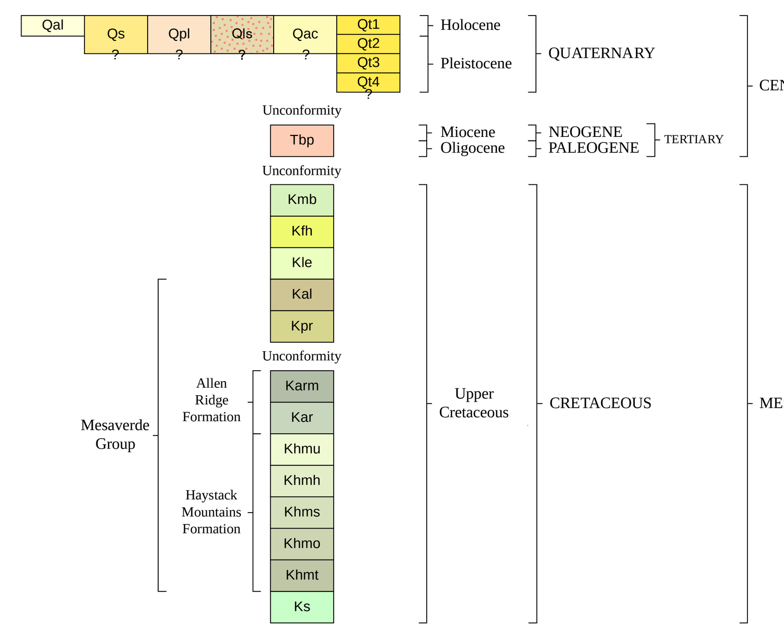

MAP SYMBOLS

Definitions: *Certain—Estimated location <25 m (82 ft)*
Approximate—Estimated location 25–100 m (82–330 ft)
Inferred—Estimated location >100 m (330 ft)

Formation contact—Continuous where certain, long dash where approximate, short dash where inferred, queried where identity or existence uncertain

Fault—Continuous where certain, long dash where approximate, short dash where inferred, dotted where concealed, queried where identity or existence uncertain; bar and ball on downthrown block of normal fault, sawteeth on upper (tectonically higher) plate of thrust fault, upthrown (U) and downthrown (D) blocks designated when fault type is unknown

Anticline—Continuous where certain, long dash where approximate, dotted where concealed; arrow on end indicates direction of plunge

Overturned anticline—Continuous where certain, long dash where approximate; arrow on end indicates direction of plunge

Syncline—Continuous where certain, long dash where approximate, dotted where concealed

Overturned syncline—Long dash where approximate, dotted where concealed; arrow on end indicates direction of plunge

A A' **Line of cross section**

27 **Strike and dip of inclined bedding**

33 **Strike and dip of inclined bedding in cross-bedded rocks**

75 **Strike and dip of overturned bedding**

Strike of vertical bedding

49-007-20599 **Oil well, plugged and abandoned—**Showing API number

49-007-23293 **Gas well, plugged and abandoned—**Showing API number

49-007-20173 **Dry hole, plugged and abandoned—**Showing API number

FS-2016-Kar **Sample location—**Showing sample name for detrital zircon geochronology

REFERENCES

Anderson, J.W., 1967, Stratigraphy and depositional environments of part of the Cretaceous Mesaverde Formation north of Sinclair, Wyoming: Laramie, University of Wyoming, M.S. thesis, 89 p., 3 pls.

Blanchard, L.F., and Comstock, M.C., 1980, Geologic map and coal sections of the Pats Bottom quadrangle, Carbon County, Wyoming: U.S. Geological Survey Open-File Report 80-52, 2 sheets, scale 1:24,000.

Bowen, C.F., 1918, Stratigraphy of the Hanna Basin, Wyoming: U.S. Geological Survey Professional Paper 108-L, p. 227–235, 1 pl.

Chadeayne, D.K., 1966, The geology of Pass Creek Ridge, Saint Marys, and Cedar Ridge anticlines, Carbon County, Wyoming: Laramie, University of Wyoming, M.S. thesis, 87 p., 6 pls.

Dobbin, C.E., Bowen, C.F., and Hoots, H.W., 1929, Geology and coal and oil resources of the Hanna and Carbon basins, Carbon County, Wyoming: U.S. Geological Survey Bulletin 804, 104 p., 27 pls., scale 1:62,500.

Fox, J.E., 1971, Invertebrate fossils and environments of the Fox Hills and Medicine Bow formations (Late Cretaceous) in south-central Wyoming: Laramie, University of Wyoming, Ph.D. dissertation, 205 p.

Gill, J.R., Merewether, E.A., and Cobban, W.A., 1970, Stratigraphy and nomenclature of some Upper Cretaceous and lower Tertiary rocks in south-central Wyoming: U.S. Geological Survey Professional Paper 667, 53 p.

Martinsen, O.J., Martinsen, R.S., and Steidtmann, J.R., 1993, Mesaverde Group (Upper Cretaceous), southeastern Wyoming—Allostratigraphy versus sequence stratigraphy in a tectonically active area: American Association of Petroleum Geologists Bulletin, v. 77, no. 8, p. 1351–1373.

McClurg, T.A., 1990, Lithosome relationships and depositional environment of the O'Brien Spring Sandstone (Late Cretaceous), south-central Wyoming: Laramie, University of Wyoming, M.S. thesis, 165 p.

Mellere, Donatella, and Steel, R.J., 1995, Facies architecture and sequentiality of nearshore and 'shelf' sandbodies; Haystack Mountains Formation, Wyoming, USA: Sedimentology, v. 42, p. 551–574.

Merewether, E.A., 1971, Geologic map of the Wild Horse Mountain quadrangle, Carbon County, Wyoming: U.S. Geological Survey Geologic Quadrangle Map GQ-887, scale 1:24,000.

Merewether, E.A., 1972, Geologic map of the Rawlins NW quadrangle, Carbon County, Wyoming: U.S. Geological Survey Geologic Quadrangle Map GQ-1010, scale 1:24,000.

Merewether, E.A., 1973, Geologic map of the Lone Haystack Mountain quadrangle, Carbon County, Wyoming: U.S. Geological Survey Geologic Quadrangle Map GQ-1064, scale 1:24,000.

Montagne, John, 1991, Cenozoic history of the Saratoga Valley area, Wyoming and Colorado: Contributions to Geology, v. 29, no. 1, p. 13–70, 4 pls.

Perman, R.C., 1988, Stratigraphy and sedimentology of the Lewis Shale and Fox Hills Formation in south–central Wyoming: Berkeley, University of California, Ph.D. dissertation, 274 p.

Roehler, H.W., 1990, Stratigraphy of the Mesaverde Group in the central and eastern Greater Green River Basin, Wyoming, Colorado, and Utah: U.S. Geological Survey Professional Paper 1508, 52 p., 2 pls.

WOGCC, 2017, Wyoming Oil and Gas Conservation Commission, accessed May 2017, at http://wogcc.state.wy.us/.

NOTICE TO USERS OF INFORMATION FROM THE WYOMING STATE GEOLOGICAL SURVEY

NOTICE FOR OPEN FILE REPORTS PUBLISHED BY THE WSGS

DISCLAIMERS

DESCRIPTION OF MAP UNITS

Cenozoic

Qal **Alluvium (Holocene)**—Unconsolidated to poorly consolidated, subangular to subrounded clay, silt, sand, coarse gravels, and cobbles. Igneous and metamorphic clasts are common within the North Platte River floodplain; locally derived sedimentary clasts are common along intermittent stream courses. Thickness less than 8 m (26 ft)

Qs **Sand (Holocene and Pleistocene[?])**—Unconsolidated sand dunes, silt, and clay that is frequently vegetated. Thickness less than 5 m (16 ft)

Qpl **Playa lake deposits (Holocene and Pleistocene[?])**—Unconsolidated to well-consolidated clay, silt, and evaporites with sparse vegetation in dry playa lake depressions. Thickness undetermined

Qls **Landslide debris (Holocene and Pleistocene[?])**—Blocks and slumps of locally derived bedrock from steep and unstable slopes. Most common on Cedar Ridge and generally comprised of Pine Ridge Sandstone. Thickness less than 50 m (160 ft)

Qac **Alluvium and colluvium (Holocene and Pleistocene[?])**—Unconsolidated to poorly consolidated, subangular to subrounded clay, silt, sand, gravels, and cobbles mixed with clay-rich soil; derived from local geologic units. Includes slope wash and alluvial fan deposits that coalesce with alluvium. Thickness less than 8 m (26 ft)

Terrace deposits (Holocene and Pleistocene[?])—Unconsolidated, poorly consolidated, and locally cemented silt, sand, gravel, and igneous and metamorphic cobbles located adjacent to North Platte River. Abundant rust-orange, well-rounded quartzite cobbles up to 20 cm (8 in) in diameter. Thickness generally less than 3 m (10 ft)

Qt1 3–9 m (10–30 ft) above present river level

Qt2 12–24 m (40–80 ft) above present river level

Qt3 30–43 m (100–140 ft) above present river level

Qt4 49–55 m (160–180 ft) above present river level

Tbp **Browns Park Formation (Miocene and upper Oligocene)**—Light-gray to tan, calcareous to siliceous sandstone interbedded with white pumicite and light-gray shales overlying a basal conglomerate; subdivided into lower and upper sequences (Montagne, 1991). Overlying sandstone, siltstone, and pumicite observed only as float and unconsolidated white soil. Lower sequence includes poorly exposed basal conglomerate consisting of subrounded to rounded clasts of orange-weathering quartzites as well as other metamorphic and igneous rock types in a friable, poorly sorted sandstone matrix; less than 3 m (10 ft) thick where observed. U-Pb detrital zircon geochronology (sample FS-16-Tbp) from basal conglomerate yields a maximum depositional age of 25.8±0.2 Ma (weighted mean age at 2[illegible]). Unconformably overlies all older formations. Thickness not determined

Mesozoic

Kmb **Medicine Bow Formation (Upper Cretaceous)**—Poorly exposed dark-gray carbonaceous shale interbedded with buff to yellow-gray and fine- to medium-grained sandstone, bentonite, and rare coal. Coal ranges from a few centimeters to 3 m (10 ft) or more in thickness (Fox, 1971). Iron-stained, concretionary beds with boulder-sized nodules and petrified wood fragments are common. Basal contact is conformable and mapped at distinct color change. Approximately 520 m (1,700 ft) exposed in map area; upper part of formation not exposed

Kfh **Fox Hills Formation (Upper Cretaceous)**—Tan, buff to light-gray, very fine to fine-grained sandstone interbedded with shale. Lower sandstone consists of a 3-m-thick (10 ft) sequence of alternating massive and thinly cross-bedded layers capped by a 0.6 m (2 ft) continuous layer of dark-brown calcareous concretions. Upper sandstones are typically light gray to white and massive, interbedded with nonresistant light-gray to medium-gray shale. *Baculites clinobactus* identified by Gill and others (1970). Crops out as distinct cliff on the eastern map border; very poorly exposed to the northwest. Basal contact is conformable and gradational. Approximately 60 m (200 ft) thick

Kle **Lewis Shale (Upper Cretaceous)**—Poorly exposed, valley-forming gray to dark-gray, silty to sandy claystone and shale that is occasionally interbedded with pale yellowish-gray to light-gray, very fine grained sandstones that can form low, discontinuous, vegetated ridges. Concretions are common. Gill and others (1970) describe *Baculites eliasi*, *Baculites grandis*, *Baculites baculus*, and *Baculites clinobactus* from nearby outcrops. Dad Sandstone Member does not crop out. Basal contact is conformable and gradational. Approximately 640 m (2,100 ft) thick

Mesaverde Group (Upper Cretaceous)

Kal **Almond Formation**—Light- to medium-gray or beige, fine-grained sandstones interbedded with medium- to dark-gray fissile shale, carbonaceous shale, and rare coal. Sandstones are typically 1–3 m (3–10 ft) thick and crop out as resistant, wave-rippled, iron-stained surfaces that are well exposed between nonresistant shale units. A discrete, fossil-rich, highly cemented bed occurs 5–6 m (16–20 ft) above base of the formation in the southeast portion of the Fort Steele Breaks. *Baculites reesidei* and *Baculites jenseni* identified by Gill and others (1970). Basal contact is gradational and conformable. Approximately 165 m (540 ft) thick

Kpr **Pine Ridge Sandstone**—Light-gray to white, fine-grained, highly resistant, cross-bedded sandstone that crops out near the tops of ridges. Current ripples are common. Nonmarine fossils and trace fossils are rare. Locally interbedded with thin layers of shale. Weathers to blocky, light-gray, orange, or light-pink iron-oxide-stained, massive outcrops that are often highly jointed and fractured. Rare iron-oxide boxwork fracture fill. Base is sharp and unconformable. Approximately 40–46 m (130–150 ft) thick

Allen Ridge Formation

Karm **Marine member**—Pale-yellow to light-gray lenticular sandstone bodies overlying nonresistant interbedded shale, carbonaceous shale, and rare lenticular sandstones. Sandstones are heavily bioturbated, carbonaceous, contain current and oscillation ripples, and weather tan to light red with slightly platy parting. Contrasts sharply with the well-exposed underlying main body of the Allen Ridge Formation and typically forms a steep slope beneath relatively thin, light-colored sandstones. Lower contact is sharp and conformable. Approximately 107 m (350 ft) thick

Kar **Allen Ridge Member**—Thick sequence of orange-brown, tan, and light-gray, lenticular, very fine to fine-grained sandstones interbedded with shale, carbonaceous shale, coal, and concretionary sandstone lenses. Sandstones are generally cross-bedded and commonly bioturbated with frequent rip-up clasts, soft-sediment deformation, flaser bedding, current ripples, trace fossils, and root traces. Locally abundant *Ophiomorpha*. Weathers to well-exposed blocky sandstone ridges of varying color between nonresistant, shale valleys. Basal contact is sharp and conformable. Approximately 290–305 m (960–1,000 ft) thick

Haystack Mountains Formation—Consists of five members that each coarsen upward from marine shale to shallower marine sandstones. Previous workers (Gill and others, 1970; Merewether, 1971, 1972, 1973; Roehler, 1990; Mellere and Steel, 1995) subdivided the upper sandstone of each member from the lower shale, formally naming the sandstones but not the shales. Because the transitions from the underlying shales to the overlying sandstones are gradational, this map groups the full coarsening-upward sequence as a single member and removes the name "sandstone" from the member name (for example, Hatfield Sandstone Member is here termed Hatfield Member)

Khmu **Upper member**—Resistant, gray to tan, fine-grained sandstone lens that crops out as a discontinuous ridge 15 m (50 ft) thick within a nonresistant shale valley. Thin, slightly concretionary sandstone weathers orange to tan and contains interbedded layers of intense bioturbation, thin cross-beds, simple trace fossils, and swaley bedding; *Baculites perplexus* identified by Anderson (1967) and Gill and others (1970). Correlates to the upper unnamed member of Gill and others (1970) and to the upper unnamed and upper unnamed sandstone members of Merewether (1972, 1973, respectively). Lower contact is sharp and conformable. Approximately 115–125 m (380–410 ft) thick

Khmh **Hatfield Member**—Light-gray to yellow-gray, very fine to fine-grained cliff-forming sandstones interbedded with thin shale beds. Consists of two coarsening-upward sequences; upper sandstone weathers to a conspicuous white, highly resistant cliff above lower, blocky, yellow sandstone separated by poorly exposed shale. Sandstones contain layers of abundant trace fossils (*Schaubcylindrichnus coronus*, *Ophiomorpha*, *Planolites*[?]), bioturbation, oscillation ripples, and small- to large-scale cross-bedding. Bivalve fossils and molds are common in the lower sandstone; *Baculites asperiformis* identified by Gill and others (1970). Lower contact is sharp and conformable. Approximately 100–130 m (330–420 ft) thick

Khms **Seminoe Member**—Series of three cliff-forming, light-gray to yellow-tan, very fine to fine-grained, resistant sandstone tongues interbedded with shale and carbonaceous shale of varying thicknesses. Upper sandstone weathers to a prominent 46-m-thick (150 ft), light-gray cliff with basal cross-beds as thick as 6 m (20 ft); locally contains bivalve molds, intense bioturbation, and trace fossils (*Schaubcylindrichnus coronus*, *Ophiomorpha*). Oscillation and interference ripples are common. Lower sandstones are yellow to gray-tan in color, thinly bedded with alternating layers of cross-bedding and bioturbation, and coalesce to form a resistant ridge below the upper sandstone. *Baculites mclearni* identified in mudstone by Gill and others (1970). Correlates to the middle unnamed member of Merewether (1971, 1972, 1973) and Gill and others (1970), the Deep Creek Sandstone Member of Roehler (1990), and to the Seminoe 1, 2, 3, and 4 members of Mellere and Steel (1995). Basal contact is sharp and conformable. Approximately 220–260 m (720–860 ft) thick

Khmo **O'Brien Spring Member**—Gray-brown, very fine to fine-grained sandstone that is locally glauconitic overlying dark-gray to brownish-gray shale and carbonaceous shale. Sandstone weathers to a thinly bedded brown-gray resistant cliff with platy parting; contains *Baculites obtusus* (Gill and others, 1970) and abundant simple trace fossil burrows including *Ophiomorpha*. Shale is silty to sandy, poorly exposed, with abundant trace fossils and siderite concretions (McClurg, 1990); contains *Baculites* sp. (weak flank ribs; Gill and others, 1970). Lower contact is sharp and conformable. Approximately 85 m (280 ft) thick

Khmt **Tapers Ranch Member**—Tan to gray, very fine to fine-grained glauconitic sandstone overlying medium-gray shale. Abundant simple trace fossil burrows and tracks in both sandstone and shale. Sandstone is heavily bioturbated and commonly cross-bedded with platy parting. Bedding surfaces yield abundant casts, molds, and mud rip-ups that are locally iron-stained. Unit contains *Baculites* sp. (smooth; Gill and others, 1970). Thins to east-southeast and becomes unmappable. Basal contact is gradational and conformable. Approximately 0–46 m (0–150 ft) thick

Ks **Steele Shale (Upper Cretaceous)**—Poorly exposed, medium- to dark-gray fissile shale interbedded with rare thin beds of very fine grained argillaceous and glauconitic siltstones and sandstones (Merewether, 1973). Contains sparse layers of gray-weathering calcareous concretions and includes several persistent bentonite beds (Gill and others, 1970). Approximately 730 m (2,400 ft) thick in the western part of the Hanna Basin (Gill and others, 1970)

GEOPHYSICAL TYPE LOG

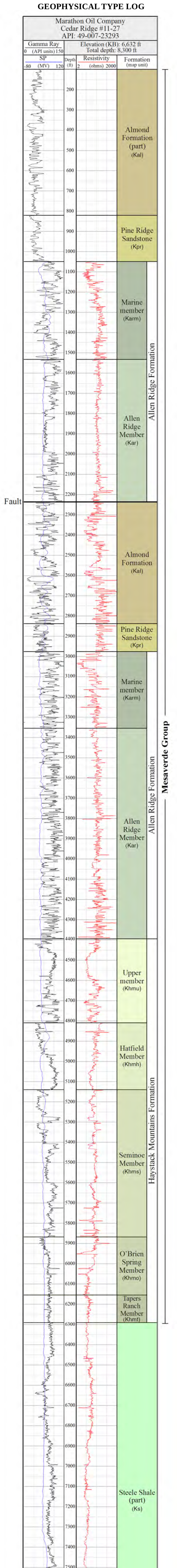

Interpreting the past, providing for the future

Preliminary Geologic Map of the Fort Steele Quadrangle, Carbon County, Wyoming

By Ranie M. Lynds and Jackie M. Wrage

Open File Report 2017-5
September 2017

Wyoming State Geological Survey

Thomas A. Drean, Director and State Geologist

Preliminary Geologic Map of the Fort Steele Quadrangle, Carbon County, Wyoming

By Ranie M. Lynds and Jackie M. Wrage

Layout by Christina D. George

Open File Report 2017-5
Wyoming State Geological Survey
Laramie, Wyoming: 2017

This Wyoming State Geological Survey (WSGS) Open File Report is preliminary and may require additional compilation and analysis. Additional data and review may be provided in subsequent years. For more information about the WSGS, or to download a copy of this Open File Report, visit www.wsgs.wyo.gov. The WSGS welcomes any comments and suggestions on this research. Please contact the WSGS at 307-766-2286, or email wsgs-info@wyo.gov.

Citation: Lynds, R.M., and Wrage, J.M., 2017, Preliminary geologic map of the Fort Steele quadrangle, Carbon County, Wyoming: Wyoming State Geological Survey Open File Report 2017-5, 25 p., scale 1:24,000.

Table of Contents

List of Figures

List of Tables

INTRODUCTION

The Fort Steele 1:24,000-scale quadrangle is located in south-central Wyoming (fig. 1) on the western margin of the Hanna Basin, east of the Rawlins Uplift. The stratigraphy of the region was first described and mapped by Veatch (1907) as part of an investigation on coal fields in Carbon County. Bowen (1918) provided the first detailed descriptions of the stratigraphy in the Hanna Basin. The quadrangle was previously mapped by Dobbin and others (1929) as part of their 1:62,500-scale geologic map of the Hanna and Carbon basins, was included in Chadeayne's (1966) geologic map of the Pass Creek (now Dana Ridge), Saint Marys, and Cedar Ridge anticlines, and was also a part of LeFebre's (1988) tectonic map of the Hanna Basin area. Other mapping nearby includes the 1:100,000-scale Rawlins quadrangle (McLaughlin and Fruhwirth, 2008) and 1:24,000-scale maps of the Rawlins NW quadrangle (Merewether, 1972), Lone Haystack Mountain quadrangle (Merewether, 1973), and Pats Bottom quadrangle (Blanchard and Comstock, 1980). Otteman and Snoke (2005) mapped the Rawlins Uplift at the scale of 1:12,000.

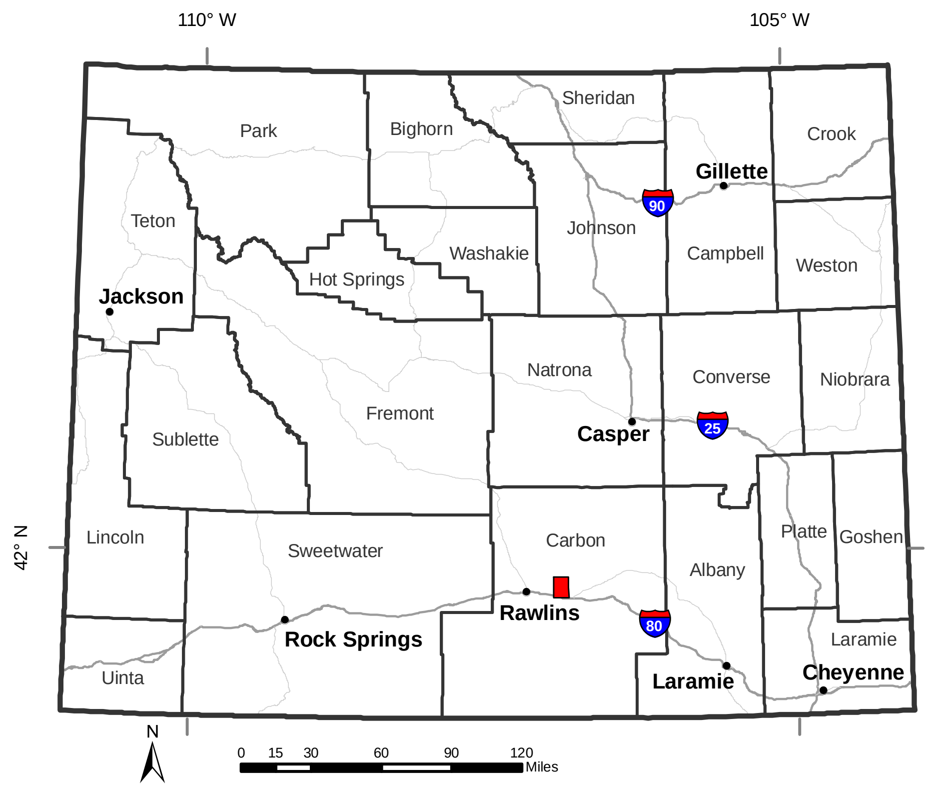

Figure 1. Map showing location of the study area in south-central Wyoming. Extent of the Fort Steele quadrangle is shown as a red box. Counties are labeled and outlined as thick black lines. U.S. highways and interstates are shown as thin light-gray and medium-gray lines, respectively.

All previous investigations within the study area are general and basin-wide, resulting in the consolidation of many of the Upper Cretaceous units. In this work, the Mesaverde Group was divided into its respective formations, and the structural aspects were explored and updated at the scale of 1:24,000.

Seventeen days of field mapping occurred during May through August 2017. Data collected in the field were integrated with satellite imagery interpretation and previous mapping and descriptions. The results were completed in cooperation with the U.S. Geological Survey 2016 StateMap grant award G16AC00199.

We gratefully acknowledge and thank the landowners and caretakers for access to their private lands. This study could not have been accomplished without their generosity.

LOCATION

The Hanna Basin is a 2,600 km^2 (1,000 mi^2) structural basin bounded by the Rawlins Uplift on the west, the Ferris, Seminoe, Shirley, and Freezeout mountains on the north, Simpson Ridge on the east, and the Medicine Bow Mountains on the south. A relatively narrow but extremely deep depression, the Hanna Basin contains more than 14 km (9 mi) of sedimentary rocks ranging in age from Cambrian to Neogene (Lillegraven, 2015) and represents the accentuated northwestward extension of the broad intermontane Laramie Basin Syncline (Dobbin and others, 1929).

The climate of the area is characterized by low precipitation, rapid evaporation, and a wide range of temperatures with an average annual precipitation in Rawlins of 28.6 cm (11.3 in; Berry, 1960). Average annual wind speeds are 28 km/hr (17 mi/hr) in the winter and 15 km/hr (9 mi/hr) in the summer (Martner and Marwitz, 1982).

The Fort Steele 7.5' quadrangle (Tps. 21 and 22 N., Rs. 84 and 85 W.), on the western rim of the Hanna Basin, is entirely within Carbon County, Wyoming. The western edge of the quadrangle is 19 km (12 mi) east of Rawlins. U.S Interstate 80 (I-80 or Interstate 80) runs northwest-southeast through the southwest corner of the quadrangle, and the Overland Route of the Union Pacific Railroad transects the southern portion of the map. The North Platte River enters the study area from the south and exits the map area on the western edge. Saint Marys Creek is an intermittent stream channel that enters the quadrangle in the southeast and flows northwest to join the North Platte River at the Fort Steele Historical Site. The Fort Steele 7.5' quadrangle is accessible from the south by Interstate 80 via exit 235 Walcott Junction (Carbon County Road 347) and exit 228 Fort Steele Rest Area. The map area is also accessible from the southeast by U.S. Highways 287/30 via the Lincoln Highway.

The quadrangle is within an area where ownership alternates every section between public land operated primarily by the Bureau of Land Management and privately held land, resulting in a checkerboard ownership pattern. Permission must be obtained from landowners prior to entering private lands.

GEOLOGIC SETTING

Strata exposed within the study area are almost exclusively Upper Cretaceous in age, deposited in the foreland basin of the Sevier orogenic belt. Although the Lower Cretaceous marine Thermopolis Shale records initiation of the Western Interior Seaway, neither the Thermopolis Shale nor the Muddy Sandstone, Mowry Shale, Frontier Formation, or Niobrara Formation are exposed within the map area. The oldest mapped unit in the quadrangle is the Upper Cretaceous deep marine Steele Shale, which was deposited during a high stand of the Western Interior Seaway. Overlying the Steele Shale, the Haystack Mountains and Allen Ridge formations record a sea level drop as the shallow marine sands and shales of the Haystack Mountains Formation grade into the fluvio-deltaic lower member of the Allen Ridge Formation. The overlying marine member of the Allen Ridge Formation records a transient period of quiescence with the deposition of thin nearshore-marine sands and shales. The Pine Ridge Sandstone unconformably caps this regressive sequence, suggesting a significant regional drop in sea level occurred pre-Pine Ridge Sandstone—followed by delta plain to fluvial deposition as sea level again began to rise (Martinsen, 1994). The coastal Almond Formation represents continuation of this second marine transgression that culminated in deposition of the Lewis Shale when the sea was at its deepest. Following the thick deposits of marine Lewis Shale, the final episode of sea level regression is recorded by the marine shoreface deposits of the Fox Hills Sandstone.

The beginning of the Laramide orogeny likely overlapped with the end of the Sevier orogeny. This period of mountain building induced the folding and faulting of sediments as well as basin segmentation and subsidence of the Sevier foreland. Accelerated subsidence in the Hanna Basin commenced in the Late Cretaceous and continued well into the Eocene (LeFebre, 1988; Lillegraven, 2015), facilitating a thick accumulation of marine and marginal marine strata that transitioned to nonmarine beginning with the Medicine Bow Formation, continued with the Ferris Formation, and ended with the Hanna Formation. Only the Medicine Bow Formation is exposed on the map area.

During the latest Oligocene and much of the Miocene, the Hanna Basin—along with the other Laramide basins in Wyoming—was filled with comingled volcanic ash, volcaniclastic sediment, and igneous and metamorphic material derived locally from adjacent uplifts. Within the study area, sediments deposited during this time correlate to the Browns Park Formation in the Saratoga Valley area (Montagne, 1991). Most of the Browns Park Formation was removed during the late Neogene following regional uplift. Pleistocene and Holocene erosion, deposition, and reworking of unconsolidated sediment is expressed as Quaternary deposits of silt, sand, and gravel in the form of sand dunes, alluvium, colluvium, and terrace gravels.

STRUCTURE

The Hanna Basin is a small Laramide basin that was tectonically segmented from the Greater Green River Basin in the early Eocene by the uplifts that define the basin boundaries. The most prominent regional structural feature is the Rawlins Uplift, a structurally complex asymmetric anticline with Precambrian rock exposed at the core, 22 km (14 mi) west of the quadrangle. The Rawlins Uplift is defined by a subsurface low-angle thrust fault that dips to the east and is responsible for 8,200 m (27,000 ft) of displacement between the basin and the core of the uplift (Otteman and Snoke, 2005).

A series of eroded anticlines and synclines expose the steeply dipping resistant Upper Cretaceous strata in the map area. The east-plunging Fort Steele Anticline is nearly symmetric, with the hinge visible in the southern part of the map area. The Steele Shale is the oldest formation exposed along the crest of the anticline, and Interstate 80 approximately parallels this fold axis. Mesaverde Group strata dip 25°–45° on both limbs. The northern limb comprises the Fort Steele Breaks, the most conspicuous topographic feature in the quadrangle that presents stunning exposures of the entire Mesaverde Group. A series of sub-vertical, strike-perpendicular faults offset strata in two locations on the Fort Steele Breaks. It is unclear if these faults are associated with folding or if they are post-Laramide relaxation faults.

The Walcott Syncline is a doubly plunging, northwest-trending asymmetric syncline that separates the Fort Steele Anticline from Cedar and Saint Marys ridges. The northeast limb of the Walcott Syncline is tightly folded and locally overturned by the Saint Marys Fault, placing older Mesaverde strata on top of the younger Lewis Shale and Medicine Bow Formation. The fault trace is poorly exposed to the northwest where it is masked by non-resistant Lewis Shale.

Saint Marys Ridge is defined by the Saint Marys Anticline, a doubly plunging asymmetric anticline that is locally overturned on the southwest limb. It is bounded by a normal fault on the northeast and by the Saint Marys Fault on the southwest. The northwest-trending normal fault down-dropped most of the northeast flank of the Saint Marys Anticline. Fault exposure is poor, but it has been well-documented to the southeast (Dobbin and others, 1929; Chadeayne, 1966), and its existence in the map area is confirmed by stratigraphic relationships and cross-section construction (cross section on map). Saint Marys Fault is a northeast-dipping thrust fault that is exposed on the southwestern part of Saint Marys Ridge as zones with multiple bands of hematite/limonite alteration and areas of significant brecciation.

The Cedar Ridge Anticline is a northwest-trending, doubly plunging anticline that forms Cedar Ridge proper. The anticline is an open fold in the northwest and terminates as a highly faulted, truncated anticline to the southeast. It is located immediately northwest of Saint Marys Ridge and is bounded by a high-angle normal fault on the northeast and by a thrust fault on the southwest. Only the hanging wall of the normal fault is exposed, where it progressively truncates the Cedar Ridge anticlinal axis to the southeast. A large slide block on the northeast side of Cedar Ridge, composed mostly of the Pine Ridge Sandstone and Almond Formation, covers the fault trace and appears to be related to this fault. The thrust fault that defines the southwest boundary of Cedar Ridge may be a northwest extension of the Saint Marys Fault. Dobbin and others (1929) only document the Saint Marys Fault while Chadeayne (1966) proposes the existence of two separate thrust faults. The interpretation presented here is the simplest explanation and is not confirmed. Subsurface data from a well on the southwest side of Cedar Ridge suggests the thrust fault continues to the northwest (type log on map) despite the lack of evidence in surface outcrops.

MINERAL ECONOMICS

Within the map area, there is potential for future oil and gas exploration with limited coal possibilities. Sand and gravel have historically been mined and are currently being mined along the North Platte River. The potential for other minerals is low, with the exception of alteration zones associated with faulting in the vicinity of Saint Marys and Cedar ridges.

Petroleum

A total of eight petroleum wells were drilled in the map area, with the most recent well completed in 2006. Table 1 shows the name, location, status, target formation, depth, and production records for these wells, which are also displayed on the map. The Wyoming Oil and Gas Conservation Commission (WOGCC, 2017) indicated production for only two of these wells, both located near the crest of the Cedar Ridge Anticline. The most productive of these wells (API 49-007-20790) produced oil for about 13 years from a sandstone within the Steele Shale.

Table 1. Oil and gas wells drilled within the boundary of the Fort Steele 7.5' quadrangle.

API	Company	Year	Location	Status	Target formation	Total depth	Produced
49-007-05516	Marathon Oil Co.	1921	NE 1/4 sec. 28, T. 21 N., R. 85 W.	PA	No record	2,250 ft	IP of water only
49-007-05535	Ft. Steele Petroleum	1944	SW 1/4 sec. 22, T. 21 N., R. 85 W.	PA	Shannon Fm.	3,640 ft	No record
49-007-05589	Marathon Oil Co.	1952	NE 1/4 sec. 22, T. 22 N., R 85 W.	PA	Sundance Fm.	13,177 ft	Dry hole
49-007-20173	BP America Production Co.	1973	NW 1/4 sec. 9, T. 21 N., R. 84 W.	PA	Madison Fm.	15,553 ft	Dry hole
49-007-20599	Byron Oil Industries Inc.	1980	NE 1/4 sec. 22, T. 22 N., R. 85 W.	PA	Niobrara Fm.	10,288 ft	16 Bbls oil
49-007-20790	Byron Oil Industries Inc.	1981	SW 1/4 sec. 15, T. 22 N., R. 85 W.	PA	Cretaceous	10,672 ft	5,317 Bbls oil
49-007-21066	Energen Resources MAQ Inc.	1985	SW 1/4 sec. 20, T. 21 N., R. 84 W.	PA	Carlile Fm.	5,176 ft	Dry hole
49-007-23293*	Marathon Oil Co.	2006	NW 1/4 sec. 27, T. 22 N., R. 85 W.	PA	Niobrara Fm.	9,781 ft	Gas only

PA – plugged and abandoned

Bbls – barrels

*Well used in type log on map

No petroleum exploration has occurred on the crest of the Saint Marys Anticline. A handful of historical wells were drilled near the crest of the Fort Steele Anticline in the Steele Shale, west of the map area. The sparse information associated with these dry hole wells suggests all were exploration wells targeting Steele Shale sands or the underlying Niobrara Formation.

Coal

Coal occurs in isolated lenses within the Allen Ridge, Almond, and Medicine Bow formations. Coal has not been mined within the map area, with the exception of an indeterminate prospect in sec. 9, T. 21 N., R. 84 W., for which historical records are unavailable (the prospect may have been mining altered fault breccia). Although coal is mined from these formations elsewhere in the region, outcrop exposures suggest a limited thickness and lateral extent of coal within the map area.

Approximately 2.8 km (1.7 mi) east of the map area, however, coal was extracted from the historic Buckley and Ryan Mine. The Buckley and Ryan Mine was within the folded beds of the Medicine Bow Formation, near the trough of the Walcott Syncline. This underground mine, located in sec. 14, T. 21 N., R. 84 W., was abandoned before 1929, although a nearby unnamed mine supplied 225 tons per year to the town of Walcott in 1929 (Dobbin and others, 1929). A single sample from the 2-m-thick (6 ft) bituminous Buckley and Ryan coal seam yielded 11.4

percent moisture, 33.8 percent volatile matter, 51.7 percent fixed carbon, 3.1 percent ash, 0.6 percent sulfur, and 11,340 Btu (sample as received from the mine; Dobbin and others, 1929).

The study area is southwest of the vast Hanna Basin coal district. The Hanna Basin mines are both underground and surface mines, with coal extraction from the overlying Ferris and Hanna formations. These formations are not exposed in the Fort Steele quadrangle.

Aggregate

Sand and gravel have been mined extensively from the alluvial channel, flood plain, and terraces adjacent to the North Platte River near the Fort Steele Historical Site. According to the Land Quality Division (2017), there is one active sand and gravel mine on the east side of the North Platte River in sec. 25, T. 21 N., R. 85 W.

Other Minerals

On the southwest flank of Saint Marys Ridge, a small abandoned pit was excavated in a highly altered zone in sec. 9, T. 21 N., R. 84 W (fig. 2a). There are two small excavations at this location, and one of them may have been prospecting for coal (fig. 2b). The purpose of this mine is not known. Otherwise, there are a few very shallow pits near zones of alteration associated with minor cross-cutting faults on both Saint Marys and Cedar ridges, but again, neither their purpose nor their findings are known. The potential for other minerals within the boundary of the quadrangle is limited.

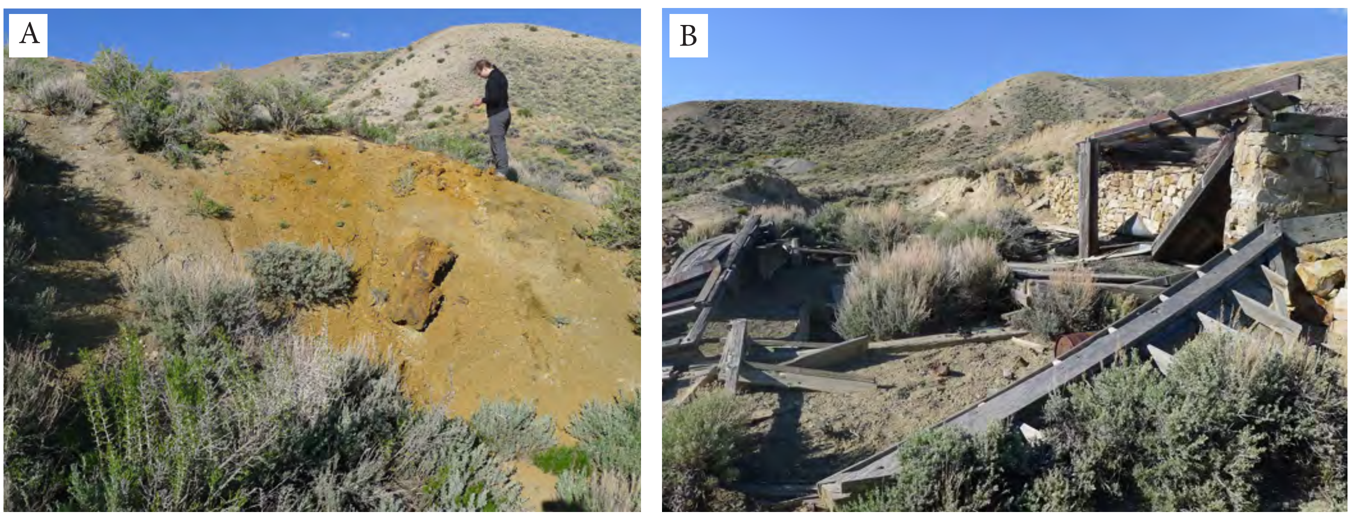

Figure 2. A) Small abandoned excavation pit on southwest flank of Saint Marys Ridge. Note high degree of hematite and limonite alteration. B) Excavation pit can be seen at the base of the hill in the upper left, abandoned building in foreground.

DESCRIPTION OF MAP UNITS

Cenozoic Deposits and Sedimentary Rocks

Quaternary

Alluvium, Holocene (Qal)

Alluvium is most common along the North Platte River and Saint Marys Creek, where it is composed of unconsolidated to poorly consolidated clay, silt, sand, coarse gravel, and cobbles. Individual clasts range from subangular to subrounded. Clasts from locally derived sedimentary units are common along intermittent stream courses while distally derived igneous and metamorphic clasts are more common within the North Platte River flood plain. The thickness of the alluvial deposits is less than 8 m (26 ft) in the study area.

Sand, Holocene and Pleistocene(?) (Qs)

Sand deposits are composed of unconsolidated sand dunes, silt, and clay that have been transported by wind. These deposits are frequently stabilized by vegetation and commonly lighter in color than the underlying formations. Vegetated areas tend to baffle the wind, causing deposition of sand and silt and allowing for vertical aggradation. The thickness of these windblown deposits is undetermined but considered less than 5 m (16 ft).

Playa lake deposits, Holocene and Pleistocene(?) (Qpl)

Dry playa lake deposits consist of unconsolidated to well-consolidated clay, silt, and evaporites. Vegetation is sparse and mud cracks are common in these low-lying areas. The presence of evaporites turns the surface of these deposits to a white crust when the climate is sufficiently dry. The thickness of playa lake deposits could not be determined from field relations.

Landslide debris, Holocene and Pleistocene(?) (Qls)

Landslide debris is composed of locally derived bedrock that collapsed or slid in blocks or slumps from steep and unstable slopes. Landslide debris is predominantly loosely consolidated slabs derived from the Pine Ridge Sandstone and the Almond Formation on Cedar Ridge. These blocks cover much of the normal fault on the northeast flank of Cedar Ridge. The thickness of landslide deposits is less than 50 m (160 ft) in the study area.

Alluvium and colluvium, Holocene and Pleistocene(?) (Qac)

Undivided alluvium and colluvium is mapped near the base of slopes and along portions of the North Platte River flood plain. This unit is made up of unconsolidated to poorly consolidated clay, silt, sand, gravel, and cobbles mixed with clay-rich soil. Clasts range from subrounded to subangular and are derived from the local geologic units. Undivided alluvium and colluvium also includes slope wash and alluvial fan deposits that coalesce with alluvium, with thicknesses generally less than 8 m (26 ft).

Terrace deposits, Holocene and Pleistocene(?) (Qt)

Terrace deposits consist of silt, sand, gravel, and cobbles ranging from unconsolidated to locally cemented units. Terraces are located adjacent to the North Platte River and represent river channel deposition established during higher water levels (fig. 3). These terraces typically form on less resistant shales as conspicuous cobble-capped hills. Cobbles consist of abundant rust-orange, well-rounded quartzite, as well as other igneous and metamorphic rock types, up to 20 cm (8 in) in diameter interpreted to have been transported from the Medicine Bow Mountains to the southeast. Four distinct levels of terrace deposits were mapped in the study area based on elevation above the present river level, including Qt1, 3–9 m (10–30 ft); Qt2, 12–24 m (40–80 ft); Qt3, 30–43 m (100–140 ft); and Qt4, 49–55 m (160–180 ft). Terrace deposits are commonly less than 3 m (10 ft) thick.

Figure 3. Terrace deposits of the Qt2 and Qt3 levels cap the broad, flat hills across the North Platte River. Unconsolidated alluvium and colluvium as well as alluvium deposits in foreground. View is to the southwest.

Paleogene and Neogene

Browns Parks Formation, Oligocene and Miocene (Tbp)

The Browns Park Formation is a light-gray to tan, calcareous to siliceous sandstone interbedded with white pumicite and light-gray shales that overlie a basal conglomerate. The formation is subdivided into upper and lower sequences (Montagne, 1991). The overlying sandstone, siltstone, and pumicite are observed only as float and unconsolidated white soil, mainly mapped on the northeast slopes of Cedar and Saint Marys ridges. The lower sequence includes a poorly exposed basal conglomerate consisting of sub-rounded to rounded clasts of orange-weathering quartzite as well as other metamorphic and igneous rock types. The conglomerate matrix is a friable, poorly sorted, locally volcaniclastic sandstone (fig. 4). This lower sequence is less than 3 m (10 ft) thick where observed in the study area and is most commonly found as a remnant near the North Platte River. U-Pb detrital zircon geochronology from the basal conglomerate (sample FS-16-Tbp, sampled north-northeast of the study area) yields a maximum depositional age of 25.8 ± 0.2 Ma (weighted mean age at 2σ; Appendix). The Browns Park Formation unconformably overlies all older formations, and the thickness could not be determined.

Figure 4. Basal conglomerate of the Browns Park Formation.

Mesozoic Sedimentary Rocks

Naming conventions of the sandstone and shale units within the lower Mesaverde Group have changed as various authors studied and mapped the units differently over the past century. Comparison between the stratigraphic units described in the present study and those described in adjacent areas is shown in figure 5.

Upper Cretaceous stages and substages		Atlantic Rim	South of Rawlins	This work	Hanna and Carbon basins
		Roehler (1990)	Mellere and Steel (1995)	Lynds and others (2017)	Merewether (1971, 1972, 1973); Gill and others (1970)
Maestrichtian	Lower	Lance Formation	Medicine Bow Formation	Medicine Bow Formation	Medicine Bow Formation
Maestrichtian	Lower	Fox Hills Sandstone	Fox Hills Formation	Fox Hills Formation	Fox Hills Formation
Maestrichtian	Lower	Lewis Shale:	Lewis Shale: Upper part	Lewis Shale	Lewis Shale: Upper part
Maestrichtian	Lower	Lewis Shale: Dad Sandstone Member	Lewis Shale: Dad Sandstone Member	Lewis Shale	Lewis Shale: Dad Sandstone Member
Maestrichtian	Lower	Lewis Shale:	Lewis Shale: Lower part	Lewis Shale	Lewis Shale: Lower part
Campanian	Upper	Mesaverde Group: Almond Formation	Almond Formation	Almond Formation	Almond Formation (Mesaverde Group)
Campanian	Upper	Mesaverde Group: Pine Ridge Sandstone	Pine Ridge Sandstone	Pine Ridge Sandstone	Pine Ridge Sandstone
Campanian	Upper	Mesaverde Group: Allen Ridge Formation	Allen Ridge Formation	Allen Ridge Fm.: marine member	Allen Ridge Fm.: marine member
Campanian	Upper	Mesaverde Group: Allen Ridge Formation	Allen Ridge Formation	Allen Ridge Fm.: Allen Ridge member	Allen Ridge Fm.: Allen Ridge member
Campanian	Upper	Haystack Mountains Formation: Unnamed sandstone mbr.	Haystack Mountains Formation: Upper unnamed member	Haystack Mountains Formation: Upper member	Haystack Mountains Formation: Upper unnamed member
Campanian	Upper	Haystack Mountains Formation: Unnamed sandstone mbr.	Haystack Mountains Formation: Hatfield 2 Member	Haystack Mountains Formation: Hatfield Member	Haystack Mountains Formation: Hatfield Sandstone Member
Campanian	Upper	Haystack Mountains Formation: Hatfield Sandstone Mbr.	Haystack Mountains Formation: Hatfield 1 Member	Haystack Mountains Formation: Hatfield Member	Haystack Mountains Formation: Hatfield Sandstone Member
Campanian	Upper	Haystack Mountains Formation: Espy Tongue	Haystack Mountains Formation: Seminoe 1, 2, 3, and 4 Mbrs.	Haystack Mountains Formation: Seminoe Member	Haystack Mountains Formation: Middle unnamed member
Campanian	Upper	Haystack Mountains Formation: Deep Creek Sandstone Mbr.	Haystack Mountains Formation: Seminoe 1, 2, 3, and 4 Mbrs.	Haystack Mountains Formation: Seminoe Member	Haystack Mountains Formation: Middle unnamed member
Campanian	Lower	Steele Shale: Cow Creek Sandstone Mbr.	Haystack Mountains Formation: O'Brien Spring Member	Haystack Mountains Formation: O'Brien Spring Member	Haystack Mountains Formation: O'Brien Spring Sandstone Mbr.
Campanian	Lower	Steele Shale: Cow Creek Sandstone Mbr.	Haystack Mountains Formation: O'Brien Spring Member	Haystack Mountains Formation: O'Brien Spring Member	Haystack Mountains Formation: Lower unnamed member
Campanian	Lower	Steele Shale: Main body	Haystack Mountains Formation: Bolten Ranch Member	Haystack Mountains Formation: Tapers Ranch Member	Haystack Mountains Formation: Tapers Ranch Sandstone Mbr.
Campanian	Lower	Steele Shale: Main body	Haystack Mountains Formation: Tapers Ranch Member	Haystack Mountains Formation: Tapers Ranch Member	Haystack Mountains Formation: Tapers Ranch Sandstone Mbr.
Campanian	Lower	Steele Shale: Main body	Steele Shale	Steele Shale	Steele Shale

Figure 5. Stratigraphy of the Upper Cretaceous units mapped in the Fort Steele quadrangle compared with the stratigraphic units described in adjacent areas (Gill and others, 1970; Merewether, 1971, 1972, 1973; Roehler, 1990; Mellere and Steel, 1995).

Cretaceous

Medicine Bow Formation, Upper Cretaceous (Kmb)

The predominantly nonmarine Medicine Bow Formation consists of dark-gray carbonaceous shale interbedded with buff to yellow-gray, fine- to medium-grained sandstone, bentonite, and rare coal. Coal beds range in thickness from centimeters to 3 m (10 ft) or more (Fox, 1971). The poorly exposed Medicine Bow Formation also includes iron-stained, concretionary beds with boulder-sized nodules. The basal contact is conformable and mapped at a distinct color change above the underlying Fox Hills Sandstone; however, this contact needs further refinement through detailed biostratigraphic correlations. The Medicine Bow Formation represents the transition from a marine to nonmarine depositional environment with the retreat of the Western Interior Seaway. Approximately 520 m (1,700 ft) of the lower portion of this unit is exposed in the map area.

Fox Hills Sandstone, Upper Cretaceous (Kfh)

The Fox Hills Sandstone is composed of two stacked sandstone bodies ranging from tan to light-gray in color and very fine to fine in grain size. The upper sandstones are typically lighter colored, massive, and are interbedded with nonresistant light-gray to medium-gray shale. The lower sandstone consists of a 3-m (10 ft) thick sequence of alternating massive and thinly cross-bedded layers capped by a 0.6 m (2 ft) continuous layer of dark-brown calcareous concretions. Gill and others (1970) identified *Baculites clinobactus* in nearby outcrops. The Fox Hills Sandstone crops out as a distinct cliff (fig. 6) on the eastern map border but is very poorly exposed in the hinge of the Walcott

Syncline due to increased alluvial and colluvial cover. The basal contact is conformable and gradational with the underlying Lewis Shale and is mapped below the first resistant sandstone when exposure is sufficient. The Fox Hills Sandstone records the retreat of the Western Interior Seaway as deposits of shoreface sands. It is approximately 60 m (200 ft) thick.

Figure 6. Outcrop of the Fox Hills Sandstone near the eastern edge of the Fort Steele quadrangle. Rocks are dipping to the northeast.

Lewis Shale, Upper Cretaceous (Kle)

The Lewis Shale is a poorly exposed silty to sandy claystone and shale that is occasionally interbedded with pale yellowish-gray to light-gray, very fine grained sandstone. This unit is nonresistant and valley-forming, commonly obscuring underlying structures. The sandstone beds can form low, discontinuous, vegetated ridges in an otherwise shallow, gently-sloping valley. Concretions are common, and Gill and others (1970) describe *Baculites eliasi*, *Baculites grandis*, *Baculites baculus*, and *Baculites clinobactus* from nearby outcrops. The conspicuous Dad Sandstone Member does not crop out in the study area. The basal contact of the Lewis Shale is conformable and gradational and is mapped above the highest continuous sandstone in the underlying Almond Formation. This formation records deposition in a deep marine environment. The Lewis Shale is approximately 700 m (2,300 ft) thick on the northwest side of the Hanna Basin (Gill and others, 1970) and approximately 640 m (2,100 ft) thick in the map area.

Mesaverde Group, Upper Cretaceous (Kal, Kpr, Karm, Kar, Khmu, Khmh, Khms, Khmo, Khmt)

Almond Formation (Kal): The Almond Formation includes light- to medium-gray or beige, fine-grained sandstones interbedded with medium- to dark-gray fissile shale, carbonaceous shale, and rare coal (fig. 7). Sandstones are typically 1–3 m (3–10 ft) thick and crop out as resistant, wave-rippled surfaces. Sandstones of the Almond Formation are frequently stained orange by iron-oxide minerals and are well exposed between the nonresistant shale units. A discrete, fossil-rich, highly cemented bed occurs 5–6 m (16–20 ft) above the base of the formation in the southeast portion of the Fort Steele Breaks (fig. 8). *Baculites reesidei* and *Baculites jenseni* were identified by Gill and others (1970) in nearby outcrops. The basal contact is gradational and conformable with the underlying Pine Ridge Sandstone, and is mapped at the transition between the platy, beige-colored sandstone and shale of the Almond Formation and the white, massive outcrops of the Pine Ridge Sandstone (fig. 9). The Almond Formation was deposited as shallow marine sands and shales in coastal to barrier plain environments during overall Western Interior Seaway transgression, although it contains numerous smaller-scale transgressive-regressive cycles (Roehler, 1990). It is approximately 165 m (540 ft) thick.

Figure 7. An outcrop of the Almond Formation near a plugged and abandoned well on Cedar Ridge (API 49-007-20790).

Figure 8. Sample of highly-cemented, fossil-rich bed of the Almond Formation in the southeast portion of the Fort Steele Breaks.

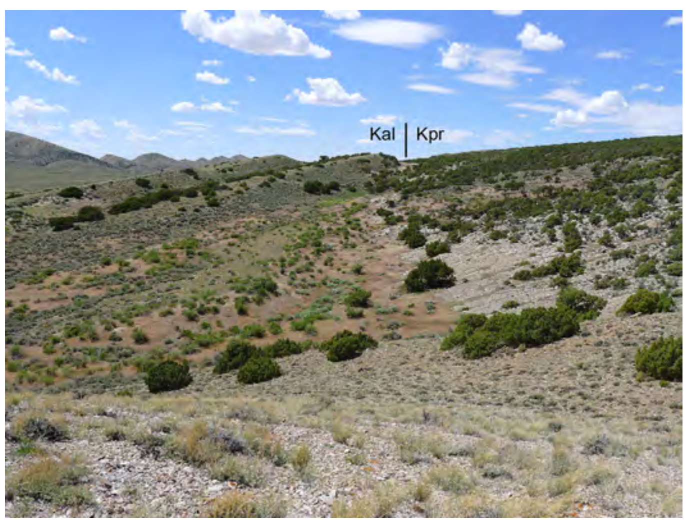

Figure 9. Contact between Almond Formation and underlying Pine Ridge Sandstone. Note the contrast between the interbedded shale and sandstone of the Almond Formation and the white, massive sandstone of the Pine Ridge Sandstone. View is to the northwest on southwest side of Cedar Ridge.

Pine Ridge Sandstone (Kpr): The Pine Ridge Sandstone is a light-gray to white, highly resistant sandstone that crops out near the tops of ridges. It is cross-bedded and contains current ripples on some bedding surfaces. The Pine Ridge Sandstone is fine grained and weathers to distinct massive outcrops that are often jointed and fractured with iron-oxide minerals staining the normally bright-white sandstone orange or light pink. More intense alteration results in rare complete infilling of fractures in the form of iron-oxide boxwork. Nonmarine fossils and trace fossils are rare, and the unit is locally interbedded with thin layers of shale. The Pine Ridge Sandstone is laterally equivalent to the Canyon Creek Member of the Ericson Formation on the Rock Springs Uplift to the west. The basal contact of the Pine Ridge Sandstone is sharp and unconformable with the underlying Allen Ridge Formation. This formation represents deposition by a network of freshwater stream channels in an alluvial plain (Roehler, 1990) or incised valley (Martinsen, 1994) environment. It is approximately 40–46 m (130–150 ft) thick in the study area.

*Allen Ridge Formation (*Karm, Kar): The Allen Ridge Formation is composed of an upper "marine" member above a lower nonmarine member. The marine member correlates to the unnamed marine member of Merewether (1971, 1973), however, Gill and others (1970), Roehler (1990), and Mellere and Steel (1995) group the two members into one formation. Since the lithologies of the members and the contact between them are distinct in the Fort Steele quadrangle, this study maps them separately. The combined thickness of the Allen Ridge Formation in the map area is approximately 397–412 m (1,310–1,350 ft).

Marine member (Karm): The marine member of the Allen Ridge Formation is made up of pale-yellow to light-gray lenticular sandstone bodies that overlie a sequence of interbedded shale, carbonaceous shale, and rare lenticular sandstones. The sandstone bodies are resistant, carbonaceous, and heavily bioturbated. They contain current and oscillation ripples and weather tan to light red with slightly platy parting. The lower shale sequence is nonresistant and typically forms a steep slope beneath the relatively thin sandstones at the top. This member of the Allen Ridge Formation principally forms a light-colored, poorly exposed slope that contrasts sharply with the well-exposed main body of the Allen Ridge Formation (fig. 10). The lower contact is sharp and conformable. The marine member is interpreted to be deposited in a shallow, nearshore marine environment, possibly as part of a delta plain (Roehler, 1990; Martinsen, 1994). The marine member is approximately 107 m (350 ft) thick.

Figure 10. Contact between the marine and Allen Ridge members of the Allen Ridge Formation. The contact is mapped at the break in slope where the color changes from the light-colored shale of the marine member to the orange-brown sandstones of the Allen Ridge Member. View is to the southeast on Fort Steele Breaks.

Allen Ridge Member (Kar): The Allen Ridge Member is the main body of the Allen Ridge Formation and consists of a thick sequence of orange-brown, tan, and light-gray lenticular sandstones interbedded with shale, carbonaceous shale, and coal. Sandstones of the Allen Ridge Member are very fine to fine grained and are generally cross-bedded with common bioturbation, including locally abundant *Ophiomorpha*. The sandstones contain rip-up clasts, soft-sediment deformation, flaser bedding, current ripples, trace fossils, and root traces. This unit weathers to well-exposed blocky sandstone ridges of varying color between nonresistant, locally concretionary shale valleys (fig. 11). This main body of the Allen Ridge Formation is interpreted to represent nonmarine transitional environments in a tidal flat and distributary channel setting (Martinsen, 1994). The basal contact is sharp and conformable and is mapped where the orange-brown sandstones of the Allen Ridge Member transition to the light-colored sandstones of the underlying Haystack Mountains Formation. This member is approximately 290–305 m (960–1,000 ft) thick in the study area.

Figure 11. Typical exposure of the Allen Ridge Member of the Allen Ridge Formation. View is to the northwest on Fort Steele Breaks.

Haystack Mountains Formation (Khmu, Khmh, Khms, Khmo, Khmt): The Haystack Mountains Formation consists of five members that each coarsen upward from marine shale to shallower marine sandstones (fig. 12). Previous workers (Gill and others, 1970; Merewether, 1971, 1972, 1973; Roehler, 1990; Mellere and Steel, 1995) subdivided the upper sandstone of each member from the lower shale, giving the sandstone units formal member names but not the shales. Because the transitions from the underlying shales to the sandstones are gradational, this map groups the full coarsening-upward sequence as a single member and removes the term "sandstone" from the member name (for example, the Hatfield Sandstone Member is here named the Hatfield Member). The members of the Haystack Mountains Formation were deposited along marine shorelines during a major regression of the Western Interior Seaway (Roehler, 1990). The entire Haystack Mountains Formation is approximately 520–645 m (1,700–2,120 ft) thick in the map area.

Figure 12. Haystack Mountains Formation cropping out on the Fort Steele Breaks. Consists of nonresistant shale units grading upwards into resistant sandstone cliffs. View is to the northwest.

Upper member (Khmu): The upper member is composed of a gray to tan, fine-grained sandstone situated between dark-gray shales that are locally carbonaceous. The resistant but discontinuous sandstone lens crops out as a locally concretionary ridge 15 m (50 ft) thick with interbedded layers of intense bioturbation, thin cross-beds, simple trace fossils, and swaley bedding that weathers orange to tan in color. *Baculites perplexus* was identified by Anderson (1967) and Gill and others (1970). This member correlates to the upper unnamed member of Gill and others (1970), to the upper unnamed member and sandstone unit of Merewether (1972), and to the upper unnamed and unnamed sandstone members of Merewether (1973). The lower contact is sharp and conformable, and the upper member is approximately 115–125 m (380–410 ft) thick in the study area.

Hatfield Member (Khmh): The Hatfield Member is a widespread stratigraphic unit across south-central Wyoming and one of the most conspicuous units within the Haystack Mountains Formation. It consists of light-gray to yellow-gray, very fine to fine-grained sandstones interbedded with thin shale beds. Within the map area, the Hatfield Member includes two coarsening-upward sequences: an upper sandstone that weathers to a conspicuous white, resistant cliff and a lower, yellow sandstone separated by poorly exposed shale (fig. 13). The sandstones contain beds with abundant *Schaubcylindrichnus coronus*, *Ophiomorpha*, and *Planolites*(?) trace fossils, other unidentified bioturbation, oscillation ripples, and small- to large-scale cross-bedding. Bivalve fossils and molds are common in the lower sandstone, and *Baculites asperiformis* was identified by Gill and others (1970) in nearby outcrops. The lower contact is sharp and conformable, and the Hatfield Member is approximately 100–130 m (330–420 ft) thick in the map area.

Figure 13. Outcrop of the Hatfield Member of the Haystack Mountains Formation. View is to the northwest along Fort Steele Breaks.

Seminoe Member (Khms): The Seminoe Member includes a series of three cliff-forming, light-gray to yellow-tan, very fine to fine-grained sandstone units interbedded with shale and carbonaceous shale of varying thickness (fig. 14). The upper sandstone weathers to a prominent, 46-m-thick (150 ft), light-gray resistant cliff with basal cross-beds as thick as 6 m (20 ft). This unit locally contains bivalve molds, intense bioturbation, and *Schaubcylindrichnus coronus* and *Ophiomorpha* trace fossils. Oscillation and interference ripples are common on bedding surfaces. The lower two sandstone tongues are yellow to gray-tan in color and thinly bedded with alternating layers of cross-bedding and bioturbation. These two units coalesce to form a resistant ridge below the upper sandstone. Gill and others (1970) identified *Baculites mclearni* in the interbedded mudstone. The Seminoe Member correlates to the middle unnamed member of Gill and others (1970) and Merewether (1971, 1972, 1973), the Deep Creek Sandstone Member of Roehler (1990), and to the Seminoe 1, 2, 3, and 4 members of Mellere and Steel (1995). The basal contact is sharp and conformable and is mapped above the resistant sandstone of the O'Brien Spring Member. It is approximately 220–260 m (720–860 ft) thick.

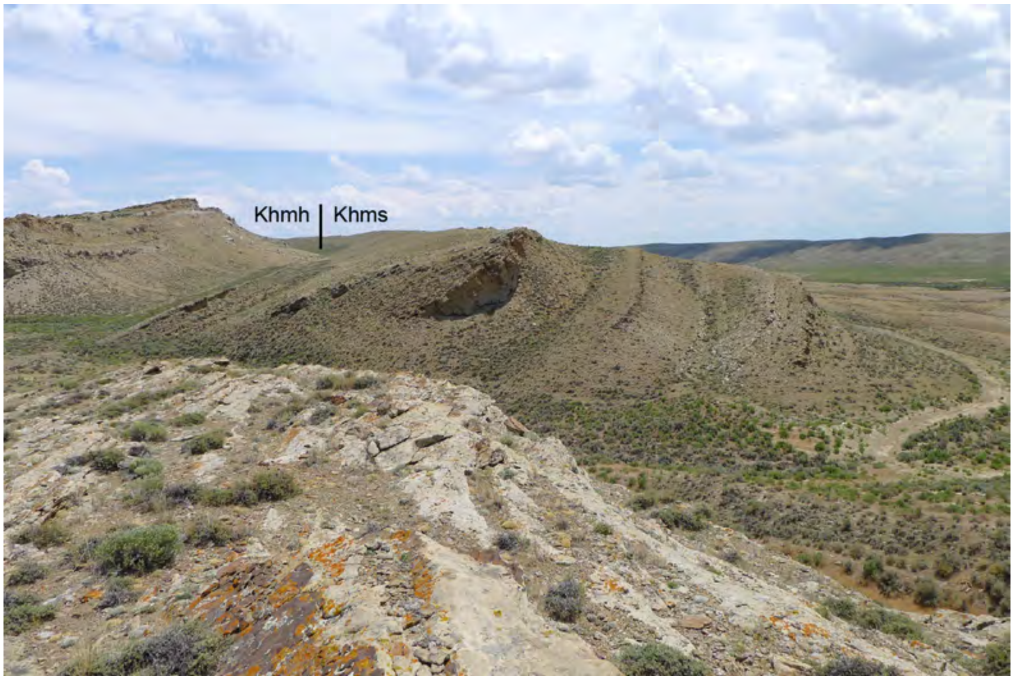

Figure 14. Hatfield and Seminoe members of the Haystack Mountains Formation. Contact is mapped at the top of the uppermost sandstone of the Seminoe Member. View is to the southeast on Fort Steele Breaks.

O'Brien Spring Member (Khmo): The O'Brien Spring Member is composed of a gray-brown, very fine to fine-grained sandstone overlying dark-gray to brownish-gray shale and carbonaceous shale. The sandstone is locally glauconitic with platy parting that weathers to a resistant, thinly bedded cliff (fig. 15). This member contains *Baculites obtusus* (Gill and others, 1970) and abundant simple trace fossil burrows, including *Ophiomorpha*. The shale is silty to sandy and poorly exposed, with abundant trace fossils and siderite concretions (McClurg, 1990) as well as *Baculites* sp. (weak flank ribs; Gill and others, 1970). The lower contact is sharp and conformable. The O'Brien Spring Member represents deposition in a more distal, lower shoreface environment than the younger members of the Haystack Mountains Formation, indicated by the presence of glauconite as well as the complete trace fossil assemblage. The O'Brien Spring Member is approximately 85 m (280 ft) thick in the map area.

Figure 15. Sandstone outcrop of the O'Brien Spring Member of the Haystack Mountains Formation. Note the dark gray-brown color and platy parting. View is to the northwest near base of Fort Steele Breaks.

Tapers Ranch Member (Khmt): The Tapers Ranch Member is a tan to gray, very fine to fine-grained glauconitic sandstone. This member contains abundant simple trace fossil burrows and tracks in both the sandstone and shale. The thinly bedded sandstone is heavily bioturbated and commonly cross-bedded with platy parting. Bedding surfaces yield abundant casts, molds, and mud rip-ups that are locally iron-stained. The Tapers Ranch Member contains *Baculites* sp. (smooth), identified by Gill and others (1970). The basal contact is gradational and conformable with the Steele Shale. Poor exposure of the Tapers Ranch Member in the study area made mapping this unit difficult, suggesting this member does not continue to the southeast. The Tapers Ranch Member was deposited in a distal shoreface environment, similar to the overlying O'Brien Spring Member. It is approximately 0–46 m (0–150 ft) thick in the study area.

Steele Shale, Upper Cretaceous (Ks): The Steele Shale is a poorly exposed, medium- to dark-gray fissile shale interbedded with rare thin beds of very fine grained argillaceous and glauconitic siltstones and sandstones (Merewether, 1973). The Steele Shale contains sparse layers of gray-weathering calcareous concretions and includes several persistent bentonite beds (Gill and others, 1970). Outcrops of this formation are restricted to terrace-capped hills adjacent to the North Platte River (fig. 16) and two very fine to fine-grained, tan to gray, glauconitic sandstone ridges that crop out in the southern portion of the map. The sandstones are moderately to highly bioturbated and contain abundant simple trace fossil tracks and burrows as well as casts, molds, and mud rip-ups on bedding surfaces, which could possibly be *Pelecypodichnus* fossils (Anderson, 1967). The Steele Shale is often mapped with the Niobrara Formation on nearby maps, but no evidence for the Niobrara Formation was observed in the Fort Steele quadrangle. Gill and others (1970) measured the thickness of the Steele Shale to be 730 m (2,400 ft) in the western part of the Hanna Basin.

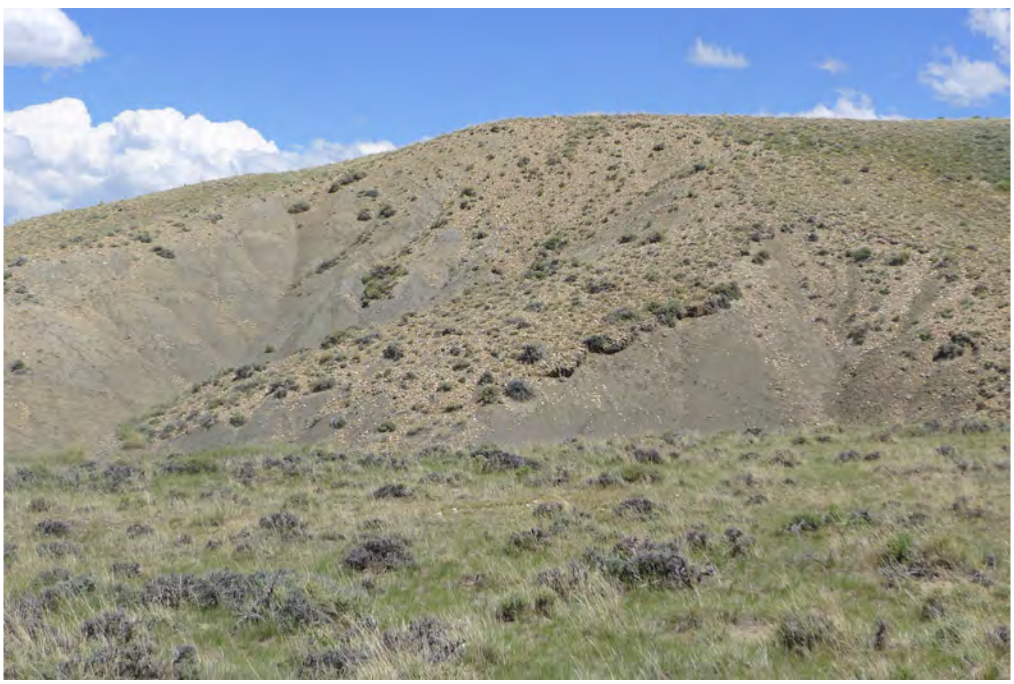

Figure 16. Outcrop of Steele Shale capped by Qt3 terrace cobbles near the North Platte River.

REFERENCES

Anderson, J.W., 1967, Stratigraphy and depositional environments of part of the Cretaceous Mesaverde Formation north of Sinclair, Wyoming: Laramie, University of Wyoming, M.S. thesis, 89 p., 3 pls.

Berry, D.W., 1960, Geology and ground-water resources of the Rawlins area, Carbon County, Wyoming: U.S. Geological Survey Water Supply Paper 1458, 74 p., 1 sheet.

Blanchard, L.F., and Comstock, M.C., 1980, Geologic map and coal sections of the Pats Bottom quadrangle, Carbon County, Wyoming: U.S. Geological Survey Open-File Report 80-52, 2 sheets, scale 1:24,000.

Bowen, C.F., 1918, Stratigraphy of the Hanna Basin, Wyoming: U.S. Geological Survey Professional Paper 108-L, p. 227–235.

Chadeayne, D.K., 1966, The geology of Pass Creek Ridge, Saint Marys, and Cedar Ridge anticlines, Carbon County, Wyoming: Laramie, University of Wyoming, M.S. thesis, 87 p., 6 pls.

Dickinson, W.R., and Gehrels, G.E., 2009, Use of U-Pb ages of detrital zircons to infer maximum depositional ages of strata—A test against a Colorado Plateau Mesozoic database: Earth and Planetary Science Letters, v. 288, p. 115–125.

Dobbin, C.E., Bowen, C.F., and Hoots, H.W., 1929, Geology and coal and oil resources of the Hanna and Carbon basins, Carbon County, Wyoming: U.S. Geological Survey Bulletin 804, 104 p., 27 pls., scale 1:62,500.

Fox, J.E., 1971, Invertebrate fossils and environments of the Fox Hills and Medicine Bow formations (Late Cretaceous) in south-central Wyoming: Laramie, University of Wyoming, Ph.D. dissertation, 205 p.

Gehrels, G.E., 2014, Detrital zircon U-Pb geochronology applied to tectonics: Annual Review of Earth and Planetary Sciences, v. 42, p. 127–149.

Gehrels, G.E., and Pecha, Mark, 2014, Detrital zircon U-Pb geochronology and Hf isotope geochemistry of Paleozoic and Triassic passive margin strata of western North America: Geosphere, v. 10, no. 1, p. 49–65.

Gehrels, G.E., Valencia, V.A., Pullen, Alex, 2006, Detrital zircon geochronology by laser-ablation multicollector ICPMS at the Arizona LaserChron Center: The Paleontological Society Papers, v. 12, p. 67–76.

Gehrels, G.E., Valencia, V.A., Ruiz, Joaquin, 2008, Enhanced precision, accuracy, efficiency, and spatial resolution of U-Pb ages by laser ablation-multicollector-inductively coupled plasma-mass spectrometry: Geochemistry, Geophysics, Geosystems, v. 9, no. 3, 13 p.

Gill, J.R., Merewether, E.A., and Cobban, W.A., 1970, Stratigraphy and nomenclature of some Upper Cretaceous and lower Tertiary rocks in south-central Wyoming: U.S. Geological Survey Professional Paper 667, 53 p.

Land Quality Division, 2017, LQD Permit Viewer: Wyoming Department of Environmental Quality, accessed August 2017, at https://gis.deq.wyoming.gov/maps/lqd_permit_public/index.html.

LeFebre, G.B., 1988, Tectonic evolution of Hanna Basin, Wyoming—Laramide block rotation in the Rocky Mountain Foreland: Laramie, University of Wyoming, Ph.D. dissertation, 240 p., 2 pls., scale 1:100,000.

Lillegraven, J.A., 2015, Late Laramide tectonic fragmentation of the eastern Greater Green River Basin, Wyoming: Rocky Mountain Geology, v. 50, no. 1, p. 30–118.

Martinsen, O.J., 1994, Evolution of an incised-valley fill, the Pine Ridge Sandstone of southeastern Wyoming, U.S.A.—Systematic sedimentary response to relative sea-level change, *in* Dalrymple, R.W., Boyd, Ron, and Zaitlin, B.A., eds., Incised-valley systems—Origin and sedimentary sequences: SEPM, Special Publication 51, p. 109–128.

Martner, B.E., and Marwitz, J.D., 1982, Wind characteristics in southern Wyoming: Journal of Applied Meteorology, v. 21, p. 1815–1827.

McLaughlin, J.F., and Fruhwirth, Jeff, 2008, Preliminary geologic map of the Rawlins 30' x 60' quadrangle, Carbon and Sweetwater counties, Wyoming: Wyoming State Geological Survey Open File Report 8-4, scale 1:100,000.

McClurg, T.A., 1990, Lithosome relationships and depositional environment of the O'Brien Spring Sandstone (Late Cretaceous), south-central Wyoming: Laramie, University of Wyoming, M.S. thesis, 165 p.

Mellere, Donatella, and Steel, R.J., 1995, Facies architecture and sequentiality of nearshore and 'shelf' sandbodies; Haystack Mountains Formation, Wyoming, USA: Sedimentology, v. 42, p. 551–574.

Merewether, E.A., 1971, Geologic map of the Wild Horse Mountain quadrangle, Carbon County, Wyoming: U.S. Geological Survey Geologic Quadrangle Map GQ-887, scale 1:24,000.

Merewether, E.A., 1972, Geologic map of the Rawlins NW quadrangle, Carbon County, Wyoming: U.S. Geological Survey Geologic Quadrangle Map GQ-1010, scale 1:24,000.

Merewether, E.A., 1973, Geologic map of the Lone Haystack Mountain quadrangle, Carbon County, Wyoming: U.S. Geological Survey Geologic Quadrangle Map GQ-1064, scale 1:24,000.

Montagne, John, 1991, Cenozoic history of the Saratoga Valley area, Wyoming and Colorado: Contributions to Geology, v. 29, no. 1, p. 13–70, 4 pls.

Otteman, A.S., and Snoke, A.W., 2005, Structural analysis of a Laramide, basement-involved, foreland fault zone, Rawlins Uplift, south-central Wyoming: Rocky Mountain Geology, v. 40, p. 65–89.

Roehler, H.W., 1990, Stratigraphy of the Mesaverde Group in the central and eastern Greater Green River Basin, Wyoming, Colorado, and Utah: U.S. Geological Survey Professional Paper 1508, 52 p., 2 pls.

Veatch, A.C., 1907, Coal fields of east-central Carbon County, Wyoming: U.S. Geological Survey Bulletin 316-D, p. 244–260.

WOGCC, 2017, Wyoming Oil and Gas Conservation Commission, accessed May 2017, at http://wogcc.state.wy.us/.

Appendix

APPENDIX: DETRITAL ZIRCON GEOCHRONOLOGY

Detrital zircon geochronology analyses were carried out at the Arizona LaserChron Center at the University of Arizona using methods described by Gehrels and Pecha (2014). U-Pb geochronology of individual zircon crystals was conducted by laser ablation multicollector inductively coupled mass spectrometry (LA-ICPMS; Gehrels and others, 2008, 2006). The isotopic analyses involved ablation of zircon using a Photon Machines Analyte G2 excimer laser coupled to a Thermo Element 2 single-collector-ICPMS. Detrital zircons from four samples were analyzed for their ratios of $^{206}Pb/^{238}U$ and $^{206}Pb/^{207}Pb$. The ratio of $^{207}Pb/^{235}U$ was then calculated from these measured ratios and the known value of $^{238}U/^{235}U$ ($^{238}U/^{235}U$ =137.82; Gehrels, 2014) to determine the age of each zircon.

Tables within this appendix summarize detrital zircon data from samples of the Allen Ridge Formation (Allen Ridge Member; FS-16-Kar), Pine Ridge Sandstone (FS-16-Kpr), Almond Formation (FS-16-Kal), and Browns Park Formation (basal conglomerate; FS-16-Tbp). The locations of samples FS-16-Kar, FS-16-Kpr, and FS-16-Kal are shown on the map, and all sample locations are summarized in table A–1. Sample FS-16-Tbp (Browns Park Formation) was collected approximately 1.6 km (1 mi) north of the quadrangle boundary.

For each sample, maximum depositional age was calculated by multiple methods following Dickinson and Gehrels (2009), with results summarized in table A–2. Youngest single grain (YSG) is the absolute youngest age measured in a sample. The probability density peak (PDP) age was calculated from the crest of the youngest discrete age peak on a probability density plot. Weighted mean age (WMA ± 2σ, incorporating both internal analytical error and external systematic error) was calculated using the DZ Age Pick Program (version of September 1, 2009) of the Arizona LaserChron Center (www.geo.arizona.edu/alc). The WMA (2σ) age was determined from the youngest cluster of three or more grain ages ($n \geq 3$) overlapping in age at 2σ by weighting each measurement by the square of its uncertainty. This method assumes the grains are cogenetic and is valid if the mean square weighted deviation (MSWD) of the set of grains is near one.

Compiled single zircon age results for the four samples summarized in table A–1 are reported in table A–3. Complete digital data are available from the WSGS (www.wsgs.wyo.gov).

Table A–1. Samples processed for detrital zircon U-Pb age dates. Latitude and longitude are displayed in GCS NAD27 and WGS84; *n* represents the number of zircons analyzed for each sample.

Sample ID	Formation	NAD27 Latitude	NAD27 Longitude	WGS84 Latitude	WGS84 Longitude	*n*
FS-16-Tbp	Tbp	41.887	-106.944	41.887	-106.945	288
FS-16-Kal	Kal	41.824	-106.978	41.824	-106.978	274
FS-16-Kpr	Kpr	41.821	-106.979	41.821	-106.979	293
FS-16-Kar	Kar	41.820	-106.985	41.819	-106.985	292

Table A–2. Maximum depositional ages (Ma) calculated by multiple methods following Dickinson and Gehrels (2009), including youngest single grain (YSG), probability density peak (PDP), weighted mean age (WMA ± 2σ (*n*), where *n* indicates the actual number of grains included in the cluster), and mean square weighted deviation (MSWD).

Sample ID	Formation	YSG	PDP	WMA (2σ)	MSWD
FS-16-Tbp	Tbp	25.2 ± 0.5	26.60	25.8 ± 0.2 (34)	1.2
FS-16-Kal	Kal	72.9 ± 1.1	73.50	75.7 ± 1.1 (3)	2.7
FS-16-Kpr	Kpr	74.1 ± 1.0	76.50	76.0 ± 0.5 (12)	1.5
FS-16-Kar	Kar	75.9 ± 1.0	78.75	78.0 ± 5.2 (3)*	—

*The mean of the youngest three ages is shown instead of the WMA (2σ) due to a high MSWD (>3).

Table A–3. Compiled detrital zircon ages (Ma; 1σ) for the four samples summarized in table A–1. Zircon ages range from Oligocene to Archean.

FS-16-Kar	FS-16-Kpr	FS-16-Kal	FS-16-Tbp
75.9 ± 1.0	74.1 ± 1.0	72.9 ± 1.1	25.2 ± 0.5
79.1 ± 1.0	74.7 ± 0.8	74.3 ± 1.1	25.2 ± 0.4
79.6 ± 1.1	75.0 ± 1.4	76.3 ± 1.5	25.3 ± 0.3
85.5 ± 1.2	75.1 ± 1.0	77.2 ± 1.2	25.5 ± 0.5
88.2 ± 1.1	75.2 ± 1.0	78.3 ± 1.2	25.6 ± 0.5
90.0 ± 1.1	75.2 ± 1.0	79.4 ± 1.3	25.7 ± 0.4
90.7 ± 1.0	75.4 ± 1.1	81.5 ± 1.0	25.8 ± 0.4
91.2 ± 1.2	75.6 ± 1.1	81.9 ± 1.2	25.8 ± 0.9
91.8 ± 1.2	76.2 ± 0.6	83.8 ± 1.1	25.8 ± 0.3
91.9 ± 1.1	76.7 ± 1.0	86.0 ± 1.1	25.9 ± 0.4
92.4 ± 1.3	76.8 ± 1.0	88.5 ± 1.0	25.9 ± 0.3
92.7 ± 1.0	77.1 ± 0.8	90.0 ± 1.2	26.0 ± 0.4
92.7 ± 1.0	77.6 ± 1.0	91.9 ± 1.3	26.0 ± 0.5
92.8 ± 1.5	78.1 ± 1.3	92.6 ± 1.1	26.2 ± 0.5
92.9 ± 1.0	78.2 ± 1.1	92.7 ± 1.0	26.4 ± 0.3
92.9 ± 1.7	80.0 ± 1.1	94.5 ± 1.4	26.6 ± 0.4
93.1 ± 1.2	86.3 ± 1.3	94.5 ± 1.0	26.8 ± 0.3
93.5 ± 1.1	86.3 ± 1.3	94.6 ± 1.5	26.8 ± 0.5
94.6 ± 1.1	87.2 ± 0.9	94.8 ± 1.2	26.9 ± 0.4
94.7 ± 1.1	91.0 ± 1.2	95.2 ± 1.5	27.0 ± 0.4
94.8 ± 1.3	91.6 ± 1.7	97.1 ± 1.5	27.1 ± 0.9
94.9 ± 0.9	91.6 ± 1.2	97.5 ± 1.1	27.2 ± 0.5
95.0 ± 1.3	91.7 ± 1.2	98.3 ± 1.3	27.2 ± 0.6
95.0 ± 1.0	91.8 ± 1.2	99.0 ± 1.9	27.5 ± 0.4
95.0 ± 1.5	92.3 ± 1.0	99.5 ± 1.5	27.6 ± 0.5
95.0 ± 1.2	93.6 ± 1.0	99.9 ± 1.5	27.8 ± 0.4
95.2 ± 1.2	93.9 ± 1.3	100.1 ± 1.2	28.1 ± 0.4
95.2 ± 1.6	94.1 ± 1.2	101.5 ± 1.2	28.1 ± 0.4
95.4 ± 1.6	94.6 ± 1.0	101.8 ± 1.3	28.2 ± 0.4
95.5 ± 1.1	95.0 ± 1.4	105.4 ± 1.4	28.3 ± 0.4
95.8 ± 1.4	95.0 ± 1.2	111.9 ± 1.5	28.6 ± 0.5
96.0 ± 1.5	95.2 ± 1.7	137.3 ± 2.4	28.9 ± 0.4
96.0 ± 1.4	95.6 ± 1.4	146.5 ± 2.1	29.0 ± 0.4
96.0 ± 1.4	95.7 ± 1.1	147.7 ± 2.2	29.1 ± 0.5
96.2 ± 1.3	95.7 ± 1.3	148.1 ± 2.1	29.5 ± 0.3
96.5 ± 1.4	95.8 ± 1.0	148.2 ± 2.3	29.9 ± 0.4
96.6 ± 1.3	95.9 ± 1.1	149.3 ± 3.1	31.5 ± 0.4
96.6 ± 1.3	96.0 ± 0.9	149.3 ± 1.3	32.4 ± 0.6
96.8 ± 1.3	96.3 ± 1.2	152.7 ± 2.2	32.8 ± 0.6
96.8 ± 1.3	96.3 ± 1.1	156.7 ± 2.9	33.7 ± 0.4

Table A–3 continued.

FS-16-Kar	FS-16-Kpr	FS-16-Kal	FS-16-Tbp
97.1 ± 1.1	96.4 ± 1.5	158.2 ± 2.7	33.7 ± 0.5
97.1 ± 1.2	96.5 ± 1.0	159.7 ± 2.4	34.3 ± 0.5
97.1 ± 1.3	96.8 ± 1.4	161.0 ± 2.1	34.3 ± 0.5
97.4 ± 1.2	96.9 ± 1.1	162.4 ± 2.1	34.4 ± 0.5
97.8 ± 1.4	97.6 ± 1.1	162.4 ± 2.1	34.8 ± 0.6
97.9 ± 1.3	98.1 ± 1.3	162.6 ± 2.4	35.1 ± 0.5
98.1 ± 1.2	98.2 ± 1.8	163.5 ± 2.1	35.2 ± 0.6
98.4 ± 1.3	98.5 ± 1.5	163.7 ± 2.1	35.2 ± 0.4
98.5 ± 1.1	98.7 ± 1.3	163.7 ± 2.5	35.2 ± 0.5
98.5 ± 1.2	98.8 ± 1.6	164.5 ± 2.5	35.3 ± 0.5
98.7 ± 1.3	99.1 ± 1.2	164.7 ± 2.3	35.6 ± 0.6
98.7 ± 1.5	99.7 ± 1.8	164.7 ± 2.2	35.7 ± 0.5
99.0 ± 1.3	100.0 ± 1.0	164.8 ± 2.4	35.8 ± 0.4
99.2 ± 1.1	100.1 ± 1.4	165.0 ± 2.4	36.0 ± 0.6
99.4 ± 1.5	100.3 ± 1.3	165.5 ± 2.2	36.0 ± 0.6
99.5 ± 1.6	101.8 ± 1.3	166.0 ± 2.1	36.1 ± 0.6
100.0 ± 1.4	102.1 ± 1.0	166.4 ± 2.0	36.2 ± 0.6
100.0 ± 1.5	102.1 ± 1.1	168.9 ± 1.8	36.2 ± 0.5
100.5 ± 1.6	102.9 ± 1.3	169.1 ± 2.0	36.4 ± 0.5
100.6 ± 1.6	103.0 ± 1.5	169.8 ± 2.3	36.5 ± 0.5
100.8 ± 1.3	112.6 ± 1.6	170.5 ± 2.7	36.9 ± 0.6
101.3 ± 1.4	148.9 ± 2.0	172.8 ± 2.8	37.1 ± 0.6
103.6 ± 1.4	153.5 ± 1.8	174.2 ± 3.3	37.3 ± 0.7
103.9 ± 1.8	162.3 ± 2.3	175.9 ± 2.4	37.4 ± 0.4
104.9 ± 1.4	164.2 ± 1.9	177.3 ± 2.3	38.1 ± 1.0
105.2 ± 1.4	165.0 ± 2.7	177.6 ± 1.9	38.4 ± 0.5
116.1 ± 1.5	252.8 ± 2.9	178.8 ± 2.6	39.3 ± 0.6
116.4 ± 1.7	305.2 ± 4.3	179.5 ± 2.9	41.2 ± 0.5
116.7 ± 1.5	317.1 ± 3.6	182.0 ± 2.7	41.9 ± 1.0
151.8 ± 2.0	327.5 ± 3.8	191.5 ± 2.5	42.9 ± 0.7
151.9 ± 1.8	368.5 ± 8.4	192.7 ± 3.3	43.7 ± 0.5
155.4 ± 1.8	370.6 ± 5.0	218.7 ± 2.5	44.5 ± 1.6
159.0 ± 1.9	374.7 ± 4.3	229.7 ± 3.4	44.5 ± 0.5
159.1 ± 1.5	379.6 ± 4.4	235.4 ± 3.9	45.5 ± 0.6
166.2 ± 2.0	391.4 ± 5.7	243.5 ± 2.9	45.6 ± 0.7
222.0 ± 10.3	394.7 ± 16.0	252.0 ± 3.0	46.6 ± 0.8
361.3 ± 4.7	401.5 ± 3.5	275.5 ± 3.2	46.7 ± 0.8
410.9 ± 5.7	402.1 ± 5.3	298.1 ± 4.1	47.0 ± 0.7
448.3 ± 5.4	402.5 ± 4.9	393.7 ± 12.0	47.1 ± 0.6
463.3 ± 6.0	402.6 ± 5.4	398.6 ± 5.1	47.4 ± 0.7

Table A–3 continued.

FS-16-Kar	FS-16-Kpr	FS-16-Kal	FS-16-Tbp
495.3 ± 7.0	402.7 ± 5.8	406.1 ± 3.7	47.5 ± 0.5
634.8 ± 7.7	411.0 ± 4.8	413.7 ± 5.8	47.7 ± 0.6
1012.5 ± 20.7	411.2 ± 5.4	429.7 ± 5.4	47.9 ± 0.6
1082.8 ± 23.9	413.3 ± 6.1	434.8 ± 6.5	48.6 ± 0.7
1096.0 ± 22.0	418.4 ± 5.1	437.3 ± 5.1	52.3 ± 0.8
1107.3 ± 20.9	418.5 ± 3.7	443.6 ± 5.3	55.6 ± 0.8
1125.1 ± 20.3	421.5 ± 5.0	445.8 ± 5.8	56.1 ± 0.8
1151.3 ± 18.5	421.6 ± 5.8	454.6 ± 5.3	57.1 ± 0.8
1184.0 ± 19.9	423.9 ± 4.8	470.1 ± 4.5	57.1 ± 0.7
1218.5 ± 21.4	432.5 ± 5.1	559.9 ± 6.8	57.7 ± 0.9
1278.3 ± 16.1	435.2 ± 5.9	613.4 ± 6.7	57.7 ± 0.9
1357.7 ± 16.5	436.3 ± 5.2	616.3 ± 10.0	57.9 ± 0.6
1361.0 ± 17.9	436.8 ± 6.1	625.3 ± 8.6	58.3 ± 0.7
1365.0 ± 16.5	450.5 ± 5.9	630.4 ± 8.8	58.3 ± 0.8
1370.8 ± 24.3	481.9 ± 5.5	631.3 ± 8.8	58.5 ± 0.9
1372.3 ± 21.2	490.0 ± 5.6	943.4 ± 27.2	59.3 ± 1.0
1379.5 ± 21.0	491.6 ± 5.8	996.4 ± 22.3	59.7 ± 0.9
1380.2 ± 17.7	543.7 ± 6.0	1017.0 ± 24.1	60.2 ± 1.0
1381.9 ± 21.7	550.9 ± 5.5	1024.2 ± 21.7	63.0 ± 1.8
1382.1 ± 21.0	551.4 ± 6.0	1045.2 ± 27.0	63.3 ± 0.7
1388.6 ± 14.9	586.5 ± 7.5	1046.0 ± 24.1	65.0 ± 0.7
1391.9 ± 18.1	592.0 ± 7.1	1054.1 ± 23.9	66.0 ± 0.9
1399.7 ± 19.4	593.4 ± 7.2	1061.5 ± 23.4	66.8 ± 1.0
1400.6 ± 21.1	594.9 ± 5.9	1067.8 ± 20.5	73.7 ± 0.7
1410.7 ± 18.6	595.1 ± 7.4	1076.2 ± 24.2	77.0 ± 0.9
1415.8 ± 17.6	608.9 ± 7.1	1078.3 ± 19.3	98.2 ± 1.5
1416.1 ± 16.0	610.3 ± 6.9	1079.0 ± 17.1	99.0 ± 1.1
1421.7 ± 18.4	629.6 ± 6.5	1087.5 ± 22.2	102.0 ± 1.4
1423.1 ± 20.8	636.6 ± 6.3	1093.2 ± 23.8	102.1 ± 1.4
1428.2 ± 20.9	958.8 ± 28.1	1094.4 ± 21.5	159.5 ± 2.8
1429.9 ± 17.6	966.9 ± 15.6	1103.3 ± 29.3	163.3 ± 2.2
1431.0 ± 14.2	969.2 ± 32.0	1111.7 ± 22.2	164.6 ± 2.1
1432.2 ± 20.3	985.5 ± 25.1	1118.2 ± 25.6	171.9 ± 1.8
1439.5 ± 20.1	986.7 ± 20.4	1131.6 ± 23.0	174.3 ± 2.3
1441.1 ± 20.3	1000.5 ± 24.3	1136.7 ± 20.5	174.3 ± 2.2
1443.0 ± 19.0	1018.8 ± 15.7	1139.1 ± 24.1	176.0 ± 2.0
1449.5 ± 22.9	1019.7 ± 18.9	1140.4 ± 23.9	176.4 ± 1.8
1451.4 ± 17.2	1021.7 ± 20.2	1159.4 ± 16.7	178.6 ± 2.7
1451.6 ± 17.4	1059.8 ± 25.0	1166.4 ± 44.4	178.6 ± 2.2
1452.9 ± 16.9	1063.0 ± 15.9	1166.5 ± 20.1	181.9 ± 1.8
1458.8 ± 17.8	1066.3 ± 16.1	1169.8 ± 21.5	193.5 ± 2.3
1458.9 ± 18.7	1081.9 ± 23.1	1172.4 ± 26.4	213.0 ± 2.5

Table A–3 continued.

FS-16-Kar	FS-16-Kpr	FS-16-Kal	FS-16-Tbp
1468.8 ± 20.0	1089.8 ± 21.8	1197.6 ± 21.9	218.1 ± 3.1
1523.6 ± 17.2	1099.4 ± 22.5	1201.2 ± 23.1	221.3 ± 2.6
1530.0 ± 20.5	1103.4 ± 19.7	1213.4 ± 19.8	226.5 ± 2.9
1623.4 ± 20.6	1103.7 ± 23.5	1216.9 ± 23.1	236.3 ± 3.5
1628.9 ± 18.6	1107.6 ± 25.3	1224.1 ± 18.5	514.6 ± 6.7
1636.0 ± 17.4	1136.4 ± 25.6	1227.6 ± 25.5	517.5 ± 6.0
1645.6 ± 23.9	1140.2 ± 15.7	1237.3 ± 23.5	520.4 ± 6.5
1657.5 ± 18.2	1141.3 ± 22.4	1244.2 ± 21.2	527.8 ± 6.5
1663.9 ± 15.2	1142.1 ± 23.9	1249.1 ± 18.8	1046.3 ± 14.0
1664.8 ± 17.8	1142.3 ± 20.7	1251.2 ± 16.7	1052.8 ± 24.5
1666.5 ± 17.4	1165.1 ± 20.6	1256.9 ± 30.0	1065.9 ± 16.6
1670.7 ± 15.0	1174.8 ± 15.8	1281.1 ± 21.2	1067.0 ± 23.4
1671.2 ± 13.8	1181.6 ± 20.9	1288.6 ± 28.7	1076.9 ± 22.8
1671.4 ± 15.7	1228.1 ± 18.2	1304.9 ± 23.2	1091.3 ± 23.5
1672.1 ± 15.8	1235.3 ± 20.4	1322.4 ± 21.7	1093.0 ± 15.5
1673.1 ± 17.0	1238.2 ± 17.3	1333.6 ± 20.4	1121.5 ± 25.8
1674.3 ± 14.1	1256.4 ± 19.5	1340.1 ± 22.0	1122.1 ± 22.1
1677.7 ± 16.5	1260.4 ± 15.3	1361.3 ± 24.5	1135.7 ± 18.9
1679.7 ± 20.5	1287.7 ± 21.7	1364.9 ± 16.5	1179.0 ± 19.3
1684.7 ± 17.5	1295.6 ± 22.8	1365.7 ± 23.9	1183.0 ± 17.3
1685.4 ± 19.4	1320.9 ± 17.1	1373.9 ± 23.1	1187.8 ± 13.4
1688.5 ± 16.3	1329.1 ± 19.6	1379.7 ± 21.1	1192.8 ± 15.2
1690.2 ± 18.9	1345.6 ± 19.2	1390.1 ± 24.4	1203.1 ± 18.6
1692.4 ± 17.4	1363.3 ± 20.3	1402.9 ± 21.2	1241.9 ± 16.1
1692.5 ± 15.6	1369.4 ± 15.7	1403.1 ± 20.3	1260.7 ± 23.7
1693.0 ± 16.9	1373.7 ± 17.8	1407.0 ± 23.2	1273.6 ± 13.6
1693.6 ± 19.0	1385.0 ± 18.1	1410.6 ± 18.6	1379.2 ± 16.9
1697.5 ± 18.7	1387.2 ± 20.7	1417.4 ± 30.0	1382.4 ± 15.8
1697.6 ± 18.8	1387.3 ± 20.2	1430.3 ± 16.5	1385.4 ± 17.5
1698.4 ± 17.7	1393.7 ± 16.6	1448.7 ± 21.4	1386.7 ± 17.8
1699.4 ± 14.6	1397.5 ± 17.1	1450.1 ± 22.5	1393.3 ± 16.7
1699.6 ± 19.1	1410.5 ± 17.1	1450.7 ± 19.9	1404.6 ± 23.5
1701.4 ± 20.5	1414.5 ± 19.0	1454.9 ± 23.9	1408.1 ± 16.6
1701.6 ± 15.0	1414.6 ± 16.7	1456.4 ± 17.6	1408.6 ± 20.2
1702.3 ± 17.9	1419.4 ± 18.5	1458.7 ± 23.9	1408.7 ± 19.2
1703.5 ± 15.1	1426.6 ± 19.4	1481.1 ± 25.4	1409.1 ± 15.9
1704.4 ± 17.0	1432.8 ± 19.7	1488.3 ± 22.3	1412.3 ± 25.0
1705.0 ± 16.5	1432.8 ± 16.8	1496.7 ± 16.7	1414.9 ± 19.1
1705.8 ± 15.4	1439.0 ± 17.9	1497.3 ± 24.3	1415.3 ± 16.0
1706.5 ± 17.2	1439.7 ± 15.8	1499.1 ± 18.3	1417.0 ± 16.1
1706.6 ± 12.5	1440.6 ± 19.5	1503.0 ± 18.1	1417.3 ± 13.6
1707.5 ± 15.6	1441.4 ± 16.5	1505.0 ± 19.4	1417.4 ± 13.4

Table A–3 continued.

FS-16-Kar	FS-16-Kpr	FS-16-Kal	FS-16-Tbp
1708.6 ± 20.1	1441.6 ± 20.1	1524.5 ± 20.3	1418.1 ± 16.6
1710.0 ± 19.0	1444.9 ± 20.3	1550.6 ± 46.5	1421.2 ± 16.9
1711.4 ± 16.9	1453.7 ± 17.6	1565.8 ± 21.6	1421.3 ± 16.5
1713.4 ± 18.5	1459.3 ± 25.1	1580.2 ± 16.6	1421.5 ± 17.2
1714.9 ± 17.9	1463.1 ± 21.1	1582.6 ± 17.0	1423.1 ± 18.4
1715.5 ± 15.5	1475.1 ± 16.1	1582.9 ± 21.5	1424.5 ± 17.5
1715.9 ± 20.8	1477.3 ± 20.0	1598.8 ± 20.8	1424.6 ± 16.7
1717.8 ± 16.3	1491.6 ± 20.8	1605.0 ± 18.8	1425.1 ± 19.1
1717.8 ± 19.4	1492.1 ± 18.3	1619.9 ± 20.8	1427.9 ± 19.2
1717.9 ± 18.5	1492.5 ± 15.7	1622.3 ± 17.6	1428.7 ± 16.0
1718.5 ± 19.1	1502.9 ± 12.9	1628.1 ± 18.6	1428.8 ± 16.3
1719.3 ± 14.0	1504.9 ± 19.9	1636.8 ± 19.2	1429.0 ± 25.4
1721.5 ± 17.4	1517.7 ± 19.4	1636.9 ± 17.1	1429.3 ± 14.6
1721.6 ± 18.8	1519.2 ± 19.2	1644.1 ± 23.5	1430.6 ± 20.5
1722.8 ± 18.1	1559.2 ± 17.8	1645.3 ± 14.6	1431.2 ± 13.8
1724.1 ± 17.0	1611.1 ± 16.2	1648.4 ± 22.2	1431.3 ± 18.9
1724.7 ± 16.4	1615.6 ± 19.0	1650.4 ± 14.2	1433.1 ± 24.1
1725.2 ± 16.4	1616.7 ± 18.5	1657.0 ± 23.1	1433.7 ± 23.6
1725.9 ± 17.0	1616.8 ± 17.1	1664.9 ± 19.9	1434.3 ± 16.6
1726.4 ± 18.5	1617.3 ± 17.4	1665.5 ± 17.1	1434.4 ± 20.9
1727.4 ± 18.9	1628.1 ± 17.6	1669.6 ± 17.1	1434.6 ± 20.8
1728.8 ± 17.4	1634.3 ± 17.7	1672.0 ± 19.0	1435.3 ± 15.5
1731.6 ± 17.6	1641.1 ± 14.2	1672.3 ± 18.3	1435.3 ± 15.1
1732.1 ± 16.6	1647.2 ± 16.4	1672.4 ± 16.5	1435.9 ± 12.1
1733.9 ± 20.8	1648.2 ± 21.5	1673.8 ± 23.3	1436.0 ± 16.0
1733.9 ± 17.7	1653.8 ± 19.6	1673.8 ± 21.9	1436.0 ± 13.4
1734.2 ± 19.1	1656.8 ± 18.9	1674.6 ± 23.3	1436.0 ± 17.9
1737.6 ± 21.2	1658.4 ± 19.7	1676.7 ± 22.1	1437.0 ± 18.7
1738.8 ± 17.1	1669.7 ± 16.8	1678.5 ± 17.2	1437.7 ± 21.5
1739.1 ± 19.8	1670.1 ± 17.5	1679.6 ± 17.3	1437.8 ± 22.9
1740.3 ± 18.0	1671.1 ± 39.4	1679.8 ± 23.4	1438.3 ± 13.9
1740.4 ± 16.6	1673.8 ± 14.1	1680.4 ± 19.6	1440.2 ± 18.9
1740.7 ± 18.2	1680.0 ± 16.7	1681.0 ± 17.6	1441.7 ± 14.3
1741.3 ± 15.5	1680.6 ± 18.4	1683.2 ± 24.6	1442.3 ± 15.2
1741.3 ± 19.2	1681.3 ± 16.8	1686.3 ± 23.0	1443.5 ± 16.9
1743.6 ± 18.3	1684.9 ± 18.0	1688.3 ± 18.6	1445.4 ± 14.7
1745.3 ± 16.2	1687.1 ± 18.9	1688.7 ± 18.9	1447.9 ± 17.4
1746.6 ± 19.5	1689.2 ± 16.7	1689.3 ± 23.7	1448.0 ± 14.0
1752.1 ± 21.0	1689.9 ± 16.7	1690.3 ± 19.5	1448.9 ± 16.0
1753.6 ± 15.4	1691.6 ± 16.9	1690.3 ± 21.3	1449.1 ± 16.8
1753.9 ± 16.6	1692.2 ± 16.7	1692.2 ± 17.1	1450.2 ± 16.4
1763.9 ± 16.3	1693.5 ± 15.3	1692.4 ± 19.2	1450.6 ± 15.6

Table A–3 continued.

FS-16-Kar	FS-16-Kpr	FS-16-Kal	FS-16-Tbp
1765.1 ± 16.5	1702.7 ± 15.8	1693.3 ± 17.4	1450.6 ± 14.2
1766.1 ± 15.1	1703.0 ± 16.8	1694.5 ± 14.6	1451.0 ± 14.9
1766.4 ± 18.4	1703.5 ± 18.8	1696.5 ± 20.5	1459.5 ± 18.6
1766.7 ± 17.7	1704.6 ± 15.6	1698.9 ± 17.9	1471.9 ± 15.8
1766.8 ± 16.4	1705.2 ± 20.7	1700.4 ± 17.3	1486.9 ± 15.5
1770.9 ± 18.3	1709.9 ± 20.1	1703.1 ± 20.2	1495.7 ± 15.5
1772.1 ± 16.9	1711.9 ± 19.0	1703.4 ± 14.3	1515.3 ± 30.2
1776.1 ± 17.2	1713.9 ± 20.7	1704.6 ± 18.2	1539.0 ± 17.6
1776.1 ± 18.8	1715.5 ± 17.5	1707.2 ± 17.8	1597.0 ± 13.8
1776.6 ± 17.8	1715.7 ± 14.4	1708.3 ± 19.1	1597.1 ± 15.9
1779.6 ± 17.4	1718.1 ± 19.3	1712.5 ± 22.6	1597.7 ± 15.6
1780.4 ± 18.6	1720.4 ± 18.6	1714.5 ± 20.2	1604.7 ± 18.1
1781.8 ± 19.9	1722.7 ± 18.7	1718.0 ± 17.5	1607.2 ± 15.2
1782.6 ± 16.3	1722.7 ± 15.1	1719.0 ± 17.8	1622.8 ± 14.8
1782.8 ± 16.4	1723.2 ± 18.4	1721.2 ± 23.2	1622.8 ± 15.6
1783.4 ± 18.2	1724.4 ± 19.1	1726.4 ± 16.8	1637.7 ± 15.3
1783.8 ± 13.2	1725.5 ± 15.3	1729.0 ± 17.0	1651.3 ± 15.1
1784.8 ± 16.1	1726.8 ± 16.6	1731.4 ± 17.4	1651.5 ± 16.0
1787.1 ± 20.7	1727.9 ± 16.7	1732.9 ± 19.7	1654.1 ± 16.3
1787.5 ± 16.0	1729.0 ± 13.1	1733.5 ± 20.0	1659.1 ± 17.3
1790.7 ± 16.9	1735.3 ± 16.5	1739.4 ± 19.4	1659.3 ± 18.2
1791.0 ± 16.8	1735.4 ± 12.7	1739.6 ± 20.3	1659.4 ± 13.8
1791.8 ± 21.1	1736.4 ± 16.3	1740.7 ± 16.0	1663.2 ± 24.8
1794.4 ± 18.7	1740.5 ± 14.1	1742.4 ± 22.1	1663.3 ± 14.6
1796.6 ± 17.8	1741.9 ± 15.1	1743.0 ± 22.1	1666.0 ± 17.3
1796.7 ± 16.8	1742.4 ± 22.2	1744.5 ± 21.4	1666.8 ± 17.7
1797.4 ± 17.4	1742.6 ± 15.7	1746.2 ± 17.7	1668.4 ± 13.9
1797.4 ± 17.9	1743.7 ± 13.5	1746.8 ± 20.5	1668.5 ± 17.2
1809.6 ± 17.8	1745.4 ± 16.2	1747.2 ± 20.2	1669.2 ± 16.5
1812.1 ± 17.1	1748.3 ± 16.2	1747.7 ± 23.4	1669.7 ± 16.6
1813.2 ± 16.7	1749.5 ± 14.8	1749.6 ± 19.7	1674.0 ± 14.9
1815.5 ± 25.0	1753.1 ± 19.2	1750.5 ± 19.5	1674.1 ± 13.9
1816.0 ± 16.9	1753.9 ± 19.2	1751.0 ± 16.6	1674.9 ± 14.1
1816.1 ± 16.5	1756.4 ± 18.4	1752.9 ± 16.3	1675.1 ± 14.2
1817.0 ± 17.9	1757.8 ± 18.2	1756.4 ± 14.8	1675.9 ± 13.7
1823.6 ± 17.8	1761.1 ± 18.4	1756.5 ± 17.0	1676.3 ± 14.9
1827.0 ± 17.9	1763.4 ± 16.3	1757.6 ± 22.3	1676.5 ± 16.3
1830.7 ± 23.2	1767.2 ± 15.8	1757.8 ± 21.6	1681.6 ± 15.4
1847.5 ± 19.1	1770.8 ± 16.1	1759.3 ± 19.9	1683.1 ± 16.5
1852.6 ± 14.9	1771.5 ± 15.6	1769.2 ± 18.3	1690.3 ± 14.1
1870.3 ± 20.5	1784.2 ± 15.4	1770.4 ± 21.5	1690.6 ± 14.8
1880.0 ± 38.5	1786.5 ± 16.4	1775.8 ± 18.9	1691.8 ± 14.6

Table A–3 continued.

FS-16-Kar	FS-16-Kpr	FS-16-Kal	FS-16-Tbp
1920.7 ± 19.6	1790.9 ± 17.7	1779.4 ± 18.3	1695.0 ± 12.1
1925.2 ± 16.7	1791.3 ± 17.0	1783.2 ± 17.2	1699.3 ± 16.3
1926.8 ± 17.2	1796.1 ± 19.2	1790.7 ± 17.6	1701.1 ± 14.9
1940.5 ± 19.1	1810.8 ± 19.0	1791.1 ± 17.2	1701.6 ± 16.0
1972.1 ± 17.6	1814.6 ± 13.7	1795.8 ± 21.9	1705.7 ± 20.3
1984.2 ± 15.3	1822.6 ± 13.0	1805.4 ± 17.9	1708.0 ± 13.1
1996.7 ± 14.8	1822.7 ± 14.0	1827.4 ± 16.9	1710.2 ± 17.2
2057.4 ± 17.0	1828.8 ± 18.1	1838.2 ± 17.2	1713.5 ± 17.8
2082.6 ± 15.9	1832.8 ± 15.2	1843.2 ± 18.0	1715.5 ± 13.9
2090.2 ± 18.9	1834.3 ± 16.8	1859.5 ± 20.7	1718.0 ± 13.3
2208.1 ± 19.1	1842.9 ± 11.1	1881.2 ± 20.7	1721.6 ± 20.3
2368.3 ± 13.2	1861.7 ± 15.1	1889.5 ± 23.8	1728.1 ± 17.2
2422.6 ± 15.1	1868.2 ± 18.0	1946.8 ± 22.6	1728.8 ± 15.6
2427.7 ± 14.5	1872.4 ± 16.3	1961.2 ± 19.3	1729.1 ± 24.1
2436.5 ± 13.4	1881.1 ± 16.3	2068.8 ± 16.7	1736.2 ± 15.4
2441.7 ± 15.6	1881.8 ± 15.7	2113.8 ± 16.7	1737.6 ± 13.1
2445.8 ± 16.1	1882.6 ± 14.2	2426.3 ± 19.5	1741.3 ± 12.1
2460.9 ± 15.1	1929.6 ± 16.5	2580.4 ± 18.3	1749.1 ± 15.4
2465.0 ± 16.4	1952.7 ± 15.8	2584.2 ± 18.8	1753.0 ± 15.2
2478.0 ± 13.0	1987.9 ± 19.2	2625.1 ± 17.4	1762.3 ± 14.5
2481.6 ± 16.6	2073.9 ± 15.0	2638.4 ± 20.4	1770.3 ± 17.9
2501.3 ± 13.3	2089.2 ± 16.4	2676.2 ± 16.1	1779.7 ± 19.3
2505.3 ± 17.0	2099.5 ± 16.1	2682.4 ± 14.2	1791.2 ± 14.8

Table A–3 continued.

FS-16-Kar	FS-16-Kpr	FS-16-Kal	FS-16-Tbp
2531.6 ± 17.2	2115.2 ± 14.6	2685.2 ± 15.1	1843.9 ± 17.9
2535.3 ± 16.0	2154.2 ± 14.8	2936.1 ± 14.5	1864.3 ± 13.7
2587.7 ± 20.3	2165.5 ± 14.7	3073.6 ± 13.8	1888.7 ± 16.9
2647.4 ± 13.8	2192.6 ± 16.3	—	2073.9 ± 13.4
2674.0 ± 13.9	2310.2 ± 16.5	—	2084.6 ± 21.0
2677.7 ± 16.4	2413.9 ± 16.0	—	2426.6 ± 12.5
2686.6 ± 18.6	2443.2 ± 14.0	—	2452.3 ± 13.5
2694.2 ± 20.5	2444.9 ± 13.8	—	2518.7 ± 13.4
2705.9 ± 14.2	2497.4 ± 13.0	—	2580.5 ± 14.6
2725.4 ± 15.8	2524.7 ± 17.0	—	2582.2 ± 12.3
2761.6 ± 13.2	2576.0 ± 14.4	—	2614.8 ± 11.1
2775.8 ± 16.8	2581.6 ± 19.3	—	2618.3 ± 13.6
2778.0 ± 16.6	2670.0 ± 16.2	—	2627.2 ± 14.0
2811.6 ± 14.6	2704.3 ± 14.1	—	2627.4 ± 15.0
2822.0 ± 14.0	2708.5 ± 14.9	—	2678.2 ± 17.0
2822.7 ± 14.0	2710.0 ± 16.5	—	2692.9 ± 11.3
2936.5 ± 17.3	2746.0 ± 16.9	—	2725.8 ± 13.8
2964.2 ± 16.2	2753.9 ± 12.1	—	—
2978.8 ± 16.7	2796.1 ± 12.6	—	—
2993.9 ± 13.4	2803.0 ± 15.3	—	—
3115.8 ± 16.0	2822.8 ± 16.6	—	—
—	2899.5 ± 14.8	—	—